NASA Technical Memorandum 110400

Optimal Trajectories for the Helicopter in One-Engine-Inoperative Terminal-Area Operations

Robert T. N. Chen and Yiyuan Zhao

May 1996

National Aeronautics and
Space Administration

NASA Technical Memorandum 110400

Optimal Trajectories for the Helicopter in One-Engine-Inoperative Terminal-Area Operations

Robert T. N. Chen, Ames Research Center, Moffett Field, California
Yiyuan Zhao, University of Minnesota, Minneapolis, Minnesota

May 1996

National Aeronautics and
Space Administration

Ames Research Center
Moffett Field, California 94035-1000

Nomenclature

C_P	power coefficient
C_T	thrust coefficient
(C_x, C_z)	(horizontal, vertical) component of thrust coefficient
c_d	mean profile drag coefficient of rotor blades
D_f	parasite drag of the fuselage
f_e	equivalent flat plate area for fuselage
f_G	ground effect factor
g	gravitational acceleration
(h, x)	(vertical, horizontal) position
H_R	rotor hub height when the helicopter is on the ground
I_R	polar moment of inertia of the main rotor
K_{ind}	induced power factor
m	helicopter mass
m_o	reference mass
P_{OEI}	maximum OEI power available
P_{pr}	main rotor profile power
P_{req}	helicopter power required
P_s	available shaft power
P_{TO}	one engine maximum normal takeoff power
R	main rotor radius
T	main rotor thrust
$(\overline{U}_c, \overline{U}_t)$	normalized climb and tangential flow components at the main rotor
U_2	horizontal component of V_{TOSS} or V_{BLSS}
(u, w)	(horizontal, vertical) velocity components
u_x, u_z	normalized control variables
V	airspeed
V_{TOSS}	takeoff safety speed
V_{BLSS}	balked landing safety speed
V_Y	airspeed at best rate of climb
v	induced velocity in ground effect
$\overline{v}_i$	normalized uniform induced velocity of the rotor
(X_{CTO}, X_{RTO})	total runway length in (continued takeoff, rejected takeoff)
$(x_{f\cdot cto}, x_{f\cdot rto})$	airborne runway required from optimization in (continued takeoff, rejected takeoff)
β	thrust vector inclination
γ	takeoff glide slope/approach angle
η	helicopter power efficient factor
ρ	air density
σ	rotor solidity ratio
τ_p	turboshaft engine time constant
θ_w	angle between rotor wake and a vertical reference line
Ω	main rotor angular speed
( )0	initial values at engine failure
( )max	maximum value allowed
( )min	minimum value allowed

Acronyms

AEO	all engine operating
BL	balked landing
CL	continued landing
CTO	continued takeoff
FAA	Federal Aviation Administration
JAA	Joint Aviation Authority
LDP	landing decision point
OEI	one engine inoperative
RTO	rejected takeoff
TDP	takeoff decision point

Optimal Trajectories for the Helicopter in One-Engine-Inoperative Terminal-Area Operations

ROBERT T. N. CHEN AND YIYUAN ZHAO*

Ames Research Center

Summary

This paper presents a summary of a series of recent analytical studies conducted to investigate one-engine-inoperative (OEI) optimal control strategies and the associated optimal trajectories for a twin engine helicopter in Category-A terminal-area operations. These studies also examine the associated heliport size requirements and the maximum gross weight capability of the helicopter. Using an eight states, two controls, augmented point-mass model representative of the study helicopter, continued takeoff (CTO), rejected takeoff (RTO), balked landing (BL), and continued landing (CL) are investigated for both vertical-takeoff-and-landing (VTOL) and short-takeoff-and-landing (STOL) terminal-area operations. The formulation of the nonlinear optimal control problems with considerations for realistic constraints, solution methods for the two-point boundary-value problem, a new real-time generation method for the optimal OEI trajectories, and the main results of this series of trajectory optimization studies are presented. In particular, a new balanced-weight concept for determining the takeoff decision point for VTOL Category-A operations is proposed, extending the balanced-field length concept used for STOL operations.

1. Introduction

Engine failure represents a major safety concern to helicopter operations, especially in the critical flight phases of takeoff and landing to or from small, confined areas. As a result, the JAA and the FAA both certificate a transport helicopter with a gross weight of 2720 kg (6000 lb) or more as either Category-A or Category-B according to the ability to continue its operations following engine failures (refs. 1 and 2). The Category-B certification applies to either single engine or multiengine helicopters with gross weight less than 9070 kg (20,000 lb), and requires that a safe landing be possible in the event that one or all engines become inoperative. There is no requirement, however, for continued flight capability.

In contrast, Category-A certification, which applies to multi-engine transport helicopters with independent engine systems, requires that they have the capability to continue the flight with one engine inoperative (OEI). These stringent requirements, while permitting operations from rooftops and oil rigs, and flight to areas where no emergency landing sites are available, significantly restrict the payload of a Category-A transport helicopter to a value safe for continued flight as well as for landing with one engine inoperative. Typical Category-A helicopter takeoff and landing procedures are shown in figures 1 and 2, respectively, for short takeoff and landing (STOL) to or from a clear heliport and for vertical takeoff and landing (VTOL) to or from an elevated helipad. Specifically, in a takeoff flight (figs. 1(a) and 2(a)), the pilot must continue the takeoff (CTO) if an engine failure occurs at or after passing the takeoff decision point (TDP), and should land, or reject the takeoff (RTO), if an engine failure occurs at or before reaching the TDP. In a landing flight (figs. 1(b) and 2(b)), the pilot must continue the landing (CL) if an engine fails after the helicopter has passed the Landing Decision Point (LDP). The pilot may either continue or balk the landing (BL) if an engine failure occurs at or before reaching the LDP. If no engine fails, the helicopter simply proceeds with the all-engine-operating (AEO) normal takeoff or landing. In VTOL operations, confined helipads require that the helicopter land back to the original takeoff point.

The current certification process involves extensive flight tests, which are potentially dangerous, costly, and time consuming. These tests require the pilot to simulate engine failures at increasingly critical conditions. Flight manuals based on these tests tend to provide very conservative recommendations with regard to maximum takeoff weight or required runway length. Usually, a single TDP or LDP is recommended for all flight conditions. As a result, the pilot cannot trade favorable ambient conditions or less takeoff weight for a shorter runway length.

Recently, efforts were made to address these important issues. For Category-A VTOL operations, Lande (ref. 3) experimentally investigated various takeoff and landing procedures to or from oil rigs in the North Sea, including static takeoff, dynamic takeoff, straight-in landing, and

*University of Minnesota, Minneapolis, Minnesota.

sideway ascent/descent. Stevens and Vodegel (refs. 4 and 5) developed a computer program for the certification of Category-A helicopter VTOL operation. Goldenberg, Meslin, Blondino, and Williams (ref. 6), and Wood, Blondino, and Williams (ref. 7) investigated further the use of the sideway procedure initiated previously by Lande (ref. 3), for the M230 helicopter on an elevated helipad. Some theoretical investigations have also been performed. Okuno and Kawachi (ref. 8) studied VTOL OEI optimal trajectories by minimizing the touchdown impact speed in RTO, and by maximizing the minimum altitude in CTO flyout. Sharma, Zhao, and Chen (ref. 9) conducted an OEI trajectory optimization study for the sideway Category-A operation previously investigated experimentally by Lande (ref. 3), Goldenberg (ref. 6), and Wood (ref. 7). Optimal Category-A VTOL operation, including a backup takeoff procedure, was also recently investigated by Zhao, Jhemi, and Chen (ref. 10).

Research efforts were also made to better understand Category-A STOL operations. Saal and Cole (ref. 11) conducted an extensive flight test with the S76B to investigate the merit of variable TDP and V_{TOSS}. Cerbe and Reichert (ref. 12) conducted an analytical study to investigate optimal Category-A takeoff flight for the BO-105 helicopter using a static power-required field model. Okuno and Kawachi (ref. 8) studied choices of the TDP velocity and takeoff slope for runway length reduction using nonlinear optimal control theory. Zhao and Chen (ref. 13) determined Category-A takeoff trajectories of a UH-60A helicopter to minimize runway length and to maximize gross weight. Sharma (ref. 14), and Sharma, Zhao, Chen, and Hindson (ref. 15) examined optimal OEI trajectories associated with runway landing for the UH-60A helicopter. Optimal control theories have also been used to study landing procedures in autorotation after all engines fail (refs. 16–19). In addition, a new method for real-time generation of optimal trajectories was recently developed by Jhemi, Zhao, and Chen (ref. 20) for providing timely display guidance to assist the pilot in reducing his workload and to enhance the safety of Category-A operations.

The main objective of this paper is to summarize the key results of references 10, 13–15, and 20. These efforts were made to enhance the understanding of the effects of fundamental parameters associated with Category-A VTOL and STOL operations. There are four primary concerns in these studies: (1) safety, (2) payload capability, (3) heliport size, and (4) real-time generation of optimal trajectories. In the sections that follow, the helicopter modeling, the formulation of the nonlinear optimal control problems with realistic constraints considered, the solution methods for the two-point-boundary-value problem thus formulated, and the new real-time generation method for the optimal OEI trajectories are discussed. Finally, the main results of this series of trajectory optimization studies are summarized.

2. Helicopter Model and Equations of Motion

An augmented two-dimensional, point-mass model for the UH-60A helicopter, as schematically depicted in figure 3, is used for this series of trajectory optimization studies (refs. 10 and 13–15). The governing equations are summarized below:

$$m\dot{w} = mg - \rho\left(\pi R^2\right)(\Omega R)^2 C_z - \frac{1}{2}\rho f_e w\sqrt{u^2 + w^2} \tag{1}$$

$$m\dot{u} = \rho\left(\pi R^2\right)(\Omega R)^2 C_x - \frac{1}{2}\rho f_e u\sqrt{u^2 + w^2} \tag{2}$$

$$I_R\Omega\dot{\Omega} = P_S - \frac{1}{\eta}\rho\left(\pi R^2\right)(\Omega R)^3 C_P \tag{3}$$

$$\dot{h} = -w \tag{4}$$

$$\dot{x} = u \tag{5}$$

where the thrust coefficients are defined as

$$C_T = T/\rho\left(\pi R^2\right)(\Omega R)^2 \tag{6}$$

$$C_x = C_T \sin\beta \tag{7}$$

$$C_z = C_T \cos\beta \tag{8}$$

The airspeed and flightpath angle are

$$V = \sqrt{u^2 + w^2} \tag{9}$$

$$\sin\gamma = -\frac{w}{V} \tag{10}$$

Time derivatives of C_x and C_z, instead of C_x and C_z themselves, are used as control variables to avoid discontinuity at the point of engine failure. Also, first order response dynamics for the contingency power available are assumed for turboshaft engines.

$$\dot{C}_x = u_x \tag{11}$$

$$\dot{C}_z = u_z \tag{12}$$

$$\dot{P}_S = \frac{1}{\tau_p}\left(P_{OEI} - P_S\right) \tag{13}$$

Thus, in this augmented point-mass model, there are eight state variables: u, w, h, x, C_x, C_z, Ω, and P_S, and two control variables: u_x and u_z, with helicopter mass, m, and OEI power available, P_{OEI}, playing the role of control parameters. The initial OEI conditions for the

state variables are determined from the AEO takeoff or landing path immediately prior to the engine failure.

The required power coefficient, C_P, in equation (3) is calculated from the following equation:

$$C_P = C_T\sqrt{\frac{C_T}{2}}\left(K_{ind}\, f_G \bar{v}_i + \bar{U}_c\right) + \frac{1}{8}\sigma c_d \qquad (14)$$

where

$$\bar{U}_c = \frac{u\sin\beta - w\cos\beta}{\Omega R\sqrt{C_T/2}} \qquad (15)$$

$$\bar{U}_t = \frac{u\cos\beta + w\sin\beta}{\Omega R\sqrt{C_T/2}} \qquad (16)$$

and the normalized, induced velocity of the rotor, i.e., normalized with the hover mean induced velocity, is computed using

$$\bar{v}_i = \frac{1}{\sqrt{\bar{U}_t^2 + \left(\bar{U}_c + \bar{v}_i\right)^2}}, \quad \left(2\bar{U}_c + 3\right)^2 + \bar{U}t^2 > 1 \qquad (17a)$$

$$= \bar{U}_c\left(0.373\bar{U}_c^2 + 0.598\bar{U}_t^2 - 1.991\right), \quad \text{otherwise} \qquad (17b)$$

Note that the rotor speed dynamics, equation (3), in the above set of equations is based on references 21. The efficiency factor, η, in equation (3) accounts for the power losses associated with tail rotor and transmission (ref. 22). Equation (17b) from Johnson (ref. 17) is an empirical approximation to the induced velocity in the vortex-ring state. The momentum theory for the rotor induced velocity, equation (17a), and the power-required coefficient in equation (14) are discussed in detail in references 23 and 24. Also, in equation (14), the term f_G accounts for the decrease in induced velocity due to ground effect. In general, benefits of ground effect are most pronounced at hover and decrease gradually as the horizontal speed increases (ref. 25). The simple source model of Cheeseman and Benett (ref. 26) to account for ground effect in forward flight was used in this study for simplicity, although there are some refinements (refs. 27–29) to that model to include the effect of recirculation. From reference 26,

$$f_G = 1 - \frac{R^2\cos^2\theta_w}{16\left(h + H_R\right)^2} \qquad (18)$$

where

$$\cos^2\theta_w = \frac{\left(-wC_T + vC_z\right)^2}{\left(-wC_T + vC_z\right)^2 + \left(uC_T + vC_x\right)^2} \qquad (19)$$

$$v = K_{ind} v_h \bar{v}_i f_G \qquad (20)$$

The time constant associated with induced velocity dynamics is ignored because it is much smaller compared to the flight time associated with the critical phases of takeoff and landing (see, for example, ref. 25).

The aerodynamic and structural limitations of the rotor blades result in constraints on the rotor speed, the rotor thrust, and the thrust angle.

$$\Omega_{\min} \le \Omega \le \Omega_{\max} \qquad (21)$$

$$\Omega_{\min} \le \Omega \le \Omega_{\max} \qquad (22)$$

$$\beta_{\min} \le \beta \le \beta_{\max} \qquad (23)$$

The OEI contingency power ratings are defined in terms of the level and the duration. In lieu of the 30-sec/2-min ratings, i.e., a 30-sec contingency power followed by a 2-min contingency power, which were proposed in reference 30 and recently applied in reference 31, the more traditional 2.5-min/30-min power ratings were used. In this paper, we assume that the 2.5 min OEI power rating is 110% of the AEO takeoff power rating, and the 30-min OEI power rating is 105% of the AEO takeoff power. These are typical values based on existing engine data. Therefore, upon a single engine failure, the maximum available power from the operating engine is the 2.5-min power rating assumed at 1656 hp, followed by the 30-min power at 1580 hp.

In this series of studies, the UH-60A helicopter (refs. 32 and 33) was used as the example helicopter. This single rotor helicopter is powered by two T-700-GE-700 turboshaft engines. Some important parameters of this helicopter, compiled from references 27 and 33 as well as the parameters used in the optimization studies, are listed in the Appendix.

3. Energy Considerations

Before discussing the formulation of the OEI trajectory optimization problem for Category-A STOL and VTOL operations using the helicopter model and equations of motion described above, it is instructive to consider first the problem from an energy perspective.

Category-A operations involve energy management to cope with the power deficiency resulting from loss of an engine, trading various energy sources, and controlling the rate of transfer among the levels of those energy sources. Unlike fixed-wing aircraft, the helicopter has the additional rotor rotational energy source to be utilized, in addition to the usual kinetic and potential energy sources. The total energy of the helicopter is therefore given by

$$E = mgh + \frac{1}{2}mV^2 + \frac{1}{2}I_R\Omega^2 + \frac{1}{2}I_{yy}q^2 \qquad (24)$$

The last term in the above equation accounts for the energy associated with the rotation of the aircraft for the two-dimensional case considered.

The power deficiency in an OEI situation, i.e., the power available from the remaining engine(s) minus the helicopter power required, may be supplemented by a reduction in the total energy to yield

$$P_s - P_{req} = mg\dot{h} + mV\dot{V} + I_R\Omega\dot{\Omega} + I_{yy}q\dot{q} \qquad (25)$$

Conversely, in a flight condition where the available OEI power exceeds the helicopter power required, the excess power may be used to gain altitude, to increase speed, to increase the rotor speed, or to change the flight direction.

Combining equation (25) with equations (1) and (2), and noting that the power required is the sum of the power required for the main rotor, tail rotor/transmission, and the helicopter parasite-drag power, which is $(1/2)\rho f_e V^3$, i.e.,

$$P_{req} = P_{mr} + P_{tr} + P_{para}$$

the following equation for the OEI power balance is obtained.

$$P_s = (P_{mr} + P_{tr}) + \rho\pi R^2(\Omega R)^2(uC_x - wC_z) + I_R\Omega\dot{\Omega} + I_{yy}q\dot{q} \qquad (26)$$

Equation (26), which provides a more complete alternative to equation (3) by including the power associated with the change in flight direction, may be appropriate when a complete six-degree-of-freedom rigid-body helicopter model is employed in the optimization analysis.

The helicopter power-required values for level flight at sea level standard atmospheric conditions for the study helicopter with a nominal gross weight of 16,500 lb are shown in figure 4, along with the OEI contingency power available. The power-required values were calculated from the augmented point-mass model, as described in the previous section. They are compared with those from a comprehensive blade-element simulation model (ref. 33), which have previously been partially validated with flight test data of the UH-60A helicopter (ref. 34). Despite its simplicity, the augmented point-mass model matches fairly well with the blade-element model, especially in the critical low-speed region in which the OEI contingency power is deficient. The power required exhibits the familiar shape with the minimum power point located in the 70–80 kt region for the two models at the flight conditions considered. Note that the OEI contingency power becomes deficient when the airspeed is below approximately 25 kt.

The power deficiency in this critical low-speed region may be supplemented by drawing from the helicopter potential and rotor rotational energy sources as shown in the lower portion of figure 4. Shown in the figure are three average power components: a 9% drop in rotor RPM, a 25-ft drop in altitude, and a 10-kt decrease in airspeed from various speed levels for a representative 5-sec maneuver. It is interesting to note that the first two power components are roughly equivalent, and they are approximately equal to the third component at an airspeed of 35 kt. Note also that the power deficiency near hover flight conditions may be supplemented by the combined use of the drop in the rotor RPM and in altitude. Part of the energy from these two sources may also be utilized to accelerate the helicopter towards the power-excess region which begins at an airspeed of about 25 kt. The first two sources of energy may then be replenished as the airspeed increases further.

Obtaining the precise control strategy to effect the energy management, which involves the control of the level and rate of those energy sources in consonance with the available OEI power and the required power, is the purpose of the trajectory optimization as formulated in the next section.

4. Formulation of the OEI Trajectory Optimization Problem

The OEI trajectory optimization problem will be formulated below for both VTOL and STOL operations, and will involve the four elements of takeoff and landing, i.e., rejected takeoff, continued takeoff, balked landing, and continued landing. For simplicity, a representative set of nominal AEO takeoff and landing paths was first assumed. Although the choice of the AEO takeoff or landing paths can affect the optimal OEI trajectories, the method allows us to be concerned with only OEI portion of the trajectories, not with the optimization of combined AEO and OEI trajectories.

4.1 Nominal AEO Takeoff and Landing Flightpaths

A. VTOL Case– The nominal AEO takeoff and landing flightpaths are shown in figures 2(a) and 2(b), respectively. These nominal AEO paths are selected based on recommended procedures for the UH-60A and the Super Puma helicopter. In the nominal AEO takeoff path, the helicopter begins with a 5-ft hover in ground effect. This is then followed by a steady linear backup climb

(γ = 150°, V_0 = 5 kt, $\dot{V}$ = 0) to the takeoff decision point. At any point before the TDP, the horizontal location is therefore given by

$$x_0 = -\sqrt{3}(h_0 - 5) \tag{27}$$

Around the TDP, the helicopter flies vertically up briefly before climbing out.

In the nominal AEO landing, the helicopter approaches the helipad with a constant glide path angle of –6°, and a constant deceleration of –0.075 *g*. It has a speed of 35 kt at h = 100 ft and reaches zero speed at h = 25 ft. At 25 ft above the surface of the helipad, the helicopter starts to descend and lands vertically. The horizontal location is therefore given by

$$x_0 = -\frac{h_0 - 25}{\tan 6°} \tag{28}$$

B. STOL Case– The nominal AEO STOL takeoff and landing paths are shown in figures 1(a) and 1(b). For takeoff flight, use is made of Schmitz's procedure (ref. 16) for a heavily loaded helicopter. The helicopter begins with a hover in ground effect at 5 ft. It then accelerates horizontally at a constant 0.2 *g* to an airspeed V_0. At V_0, the helicopter starts a climb at a constant flightpath angle, γ_0, while maintaining the constant airspeed. During climb, the horizontal location at any point before the TDP is thus given by

$$x_0 = \frac{V_0^2}{0.4g} + \frac{h_0 - 5}{\tan\gamma_0} \tag{29}$$

For the nominal AEO STOL landing path, it is assumed, for simplicity, that the flightpath consists of steady flight at constant airspeed, constant approach flightpath angle, and 100% rotor speed.

4.2 Rejected Takeoff Flight and Continued Landing

A. VTOL– During a successful RTO, the helicopter must return to the helipad and land safely. Therefore, the optimal control problem is formulated to minimize the dispersion of touchdown points, subject to specified touchdown speed limits. With the takeoff point taken as the origin, the following performance index is to be minimized through the use of an optimal control strategy for the two control variables, u_x, u_z, in the equations of motion and state path-constraints (eqs. (1) to (23)),

$$\min \quad J = x^2\left(t_f\right) \tag{30}$$

subject to the terminal constraints:

$$h\left(t_f\right) = 0 \tag{31}$$

$$u\left(t_f\right) \le u_{\max} \tag{32}$$

$$w\left(t_f\right) \le w_{\max} \tag{33}$$

where t_f is the time at touchdown, which is to be determined. The values of the touchdown safety speeds, $u_{\max}, w_{\max}$, chosen for the study are 15 and 5 ft/sec, respectively. With a deceleration level of –0.2 *g* assumed, the stopping distance after touchdown amounts to no more than 17.5 ft.

Preliminary calculations indicate that equation (33) can be either active or inactive, depending on helicopter gross weight and initial conditions. Therefore, for consistency, equation (33) is enforced as an equality.

B. STOL Cases– Two different performance indices are considered for the rejected takeoff optimization in STOL operations. They are (1) minimum runway length, and (2) maximum takeoff weight, i.e.,

$$\min \quad J = x\left(t_f\right) \tag{34}$$

$$\min \quad J = W_0 / W \tag{35}$$

where W_0 is a fixed, reference takeoff weight.

Again, the associated optimization problems are to find the control strategies for u_x, u_z, that minimize either the performance index (eqs. (34) or (35)), subject to the equations of motion (eqs. (1)–(20)), the state path-constraints (eqs. (21)–(23)), and the terminal constraints (eqs. (31)–(33)) to achieve reasonable touchdown speeds. For the STOL cases, the safe touchdown speeds, $u_{\max}, w_{\max}$, are chosen to be 40 ft/sec, and 5 ft/sec, respectively.

The trajectory optimization problems for the continued-landing transition flight are formulated for VTOL and STOL operations similar to those for the transition flight during the rejected takeoff described above.

4.3 Continued Takeoff and Balked Landing Flight

A. VTOL– A continued OEI takeoff must be possible after the failure of an engine at any point on or after the TDP. FAA regulations specify that at the end of a CTO transition flight, the helicopter achieves (1) a minimum of 35 ft above the takeoff surface (or above the sea level in the case of oil rig operations), (2) a minimum climb rate of 100 fpm, and (3) a pre-selected takeoff safety speed, V_{TOSS}. The required terminal constraints are therefore

$$h\left(t_f\right) \ge 35 \text{ ft} \tag{36}$$

$$-w\left(t_f\right) \ge 100 \text{ fpm} \tag{37}$$

$$u(t_f) \geq U_2(W) \tag{38}$$

$$\dot{w}(t_f) = 0 \tag{39}$$

$$\dot{u}(t_f) = 0 \tag{40}$$

$$\dot{\Omega}(t_f) = 0 \tag{41}$$

Equations (39) to (41) above are added to assure that a steady-state flight condition is attained at the end of the CTO transition. Note that U_2 in equation (38) is the horizontal component of V_{TOSS}, and they are approximately equal, since the vertical velocity component $w(t_f)$ as shown in equation (37) is very small in comparison. equation (38) is included as a terminal constraint to assure consistency between the OEI transition flight and the steady OEI climb, which is a function of gross weight and is obtained from the steady-state solution of equations (1) to (3). Table 1 lists the relationship between U_2 and the maximum gross weight in steady OEI climb at the rate of 100 fpm, at the nominal rotor speed, and with P_{OEI} = 1656 hp. Further details will be discussed later.

In a continued takeoff, tradeoff exists among payload capability, heliport adjacent space requirement, and minimum altitude drop during the OEI transition flight to a steady climb. For a given gross weight, two optimization problems are therefore formulated for CTO transition flight to minimize (1) the required runway length, and (2) the altitude drop, both subject to the equations of motion (eqs. (1)–(20)), the state path-constraints (eqs. (21)–(23)), and the terminal constraints (eqs. (36)–(41)). The two performance indices are, respectively, equations (34) and (42a) shown below.

$$\max \ \min \ h(t) \tag{42a}$$

To simplify numerical solutions, the performance index (eq. (42a)) will be replaced by an approximate form given by Johnson (ref. 36):

$$\min \quad J = \int_{t_0}^{t_f} \left(H_{ref} - h\right)^q dt \tag{42b}$$

where q is an even integer and H_{ref} is a reference altitude, well above the altitude trajectory. In this paper, the values for these two parameters are: q = 6 (or 8), and $H_{ref} = h_0 + 100$ ft.

The optimization problems for balked landing (BL) are formulated in the same way as those for CTO cases; the balked landing safety speed, V_{BLSS}, is assumed to be identical to V_{TOSS}.

B. STOL– Two optimization problems are considered for the STOL continued takeoff flight. The first is the *minimum runway-length problem* using the performance index of equation (34). The second one is the *maximum takeoff weight* in transition flight, using the performance index (eq. (35)). The minimum runway-length problem involves finding the control strategies for u_x and u_z that minimize equation (34), subject to the equations of motion (eqs. (1)–(20)), the state path-constraints (eqs. (21)–(23)), and the terminal constraints (eqs. (36)–(41)). The maximum takeoff weight problem involves minimizing the performance index (eq. (35)), subject to equations (1)–(23), equations (36)–(41), and the specified runway length, i.e.,

$$x(t_f) = X_{specified} \tag{43}$$

Again, the optimization problems for the balked landing flight are formulated identically to those for the CTO case assuming $V_{BLSS} = V_{TOSS}$.

5. Methods of Solution and Numerical Results

Obtaining the optimal flight trajectories for the OEI transition flight from the point of engine failure to the establishment of a steady climb or touchdown, as formulated in the preceding section, requires that two steady-state analyses are first performed to establish initial conditions and the maximum gross weight that would permit a continued flight.

As described previously, the helicopter states at the point of engine failure on a nominal AEO takeoff or landing path are used as initial conditions for trajectory optimizations for the OEI transition flight. An assumption is made that an engine failure occurs during a steady climb or descent portion of the nominal AEO takeoff and landing flightpaths which are described in section 4.1. The maximum weight in a steady OEI climb is discussed below.

5.1 Maximum Weight in Steady OEI Climb

The OEI climb requirements determine the maximum takeoff weight which is meaningful for the whole Category-A operation. Therefore, maximum takeoff weights in the OEI climbout are examined using the steady-state equations of equations (1)–(3). There are two segments in OEI climbout as shown in figure 1. In the first segment, from an altitude of 35 ft to at least 100 ft, the helicopter must be able to maintain a minimum climb rate of 100 fpm at V_{TOSS} or V_{BLSS} with the 2.5 min OEI power. For the second segment, from 100 to 1000 ft, the

helicopter must be able to accelerate from V_{TOSS} or V_{BLSS} to V_Y and achieve a minimum rate of climb of 150 fpm at V_Y with the 30-min OEI power.

Figure 5, which is obtained from the steady-state solution of equations (1) through (3), shows the maximum weight as a function of the horizontal velocity component of V_{TOSS} (or V_{BLSS}) in a steady climb. Three sets of conditions are included: (1) $P_{OEI} = 110\%$ AEO takeoff power (1656 hp), 100 fpm climb rate, 100% rotor RPM; (2) P_{OEI} = 110%, 100 fpm climb rate, 91% RPM; and (3) P_{OEI} = 105% (1580 hp), 150 fpm climb rate, and 100% RPM. Note that the maximum weight increases as U_2 increases and reaches a peak value at V_Y, in a manner consistent with the helicopter power required curve shown in figure 3. Clearly, the helicopter must attain a higher V_{TOSS} (or V_{BLSS}) in order to be capable of carrying a larger payload in the OEI climbout. In this series of studies, the value of U_2 examined ranges from 55 to 100 ft/sec. As shown in figure 5, the helicopter flying in this range of U_2 is capable of carrying less weight with 110% power than flying at V_Y with 105% power. Therefore, the first climb segment, which is more restrictive than the second segment, determines the maximum gross weight capability in OEI climbout as listed in table 1 for a range of U_2 values.

5.2 Numerical Solution Techniques for Trajectory Optimization

The OEI trajectory optimization problems formulated in section 4 are solved numerically using the Sequential Gradient Restoration Algorithm (SGRA) developed by Miele et al. (ref. 37), and coded by Zhao (ref. 38). This algorithm provides a numerical technique to solve a general nonlinear optimal control problem subject to terminal and path constraints on states, controls, and parameters. Since the SGRA only treats equality constraints, all the inequality constraints, equations (32), (33), and (36) to (38), are transformed to equality constraints using a slack variable method (ref. 39) by adding a positive quantity on the appropriate side of the inequality.

Proper choice of normalization and scaling of variables are vital to the computational efficiency of the numerical methods and to a successful convergence of the optimization problem. A well-scaled problem is one in which a given order of magnitude change in any variable results in the same order of magnitude change in the performance index. The following normalization and scaling were found to be satisfactory: all distances are normalized by 10R, and time by $100/\Omega_0$, where Ω_0 is the nominal rotor speed. Details of the scaled helicopter-dynamic equations and constraints can be found in references 13 and 14.

Extensive trajectory optimization was conducted using different initial guesses for states, controls, and parameters. In this paper, the results shown are for the following initial guesses: all state variables are constant and equal to their initial-time values; all control variables are also constant at the point of engine failure. Convergence criteria are selected such that further iterations will not change the performance indices by more than 0.5%.

5.3 Numerical Results – Rejected Takeoff

A. VTOL– Typical control strategies and the associated optimal trajectories for several rejected-takeoff transition flights from a backup takeoff are shown in figures 6 and 7. These are solutions with the performance index of equation (30). The backup AEO takeoff conditions are: γ_0 = 150°, V_0 = 5 kt; and P_{OEI} = 1656 hp. Figure 6 shows the effect of altitude at which the OEI occurs for gross weight at 16,000 lb. At these conditions and for the range of altitudes examined, the helicopter can always achieve successful RTOs to a close proximity of the original takeoff point, within the safe touchdown speeds of 5 ft/sec vertically and 15 ft/sec horizontally. This is consistent with the OEI H-V diagram for the helicopter at 16,000 lb. However, the touchdown point was found to deviate the most from the original takeoff point when an engine failure occurs at an altitude of 40–60 ft.

Immediately after engine failure, the optimal control strategy is to rapidly tilt the thrust vector forward to its 10° limit to accelerate the aircraft. At the same time, the thrust coefficient is increased to reduce the rotor speed to its lower limit. These maneuvers reduce the power requirement significantly to accommodate the OEI power available. When engine failure occurs at a lower altitude, the vertical descent rate and airspeed both reach the safety limit values at the touchdown point. When an engine fails at a higher altitude, the helicopter has more time to develop a higher descent rate before touchdown, and the airspeed reaches its peak during the RTO transition flight. In this case, the thrust inclination is reversed (aircraft pitched up) to reduce the airspeed and sink rate to meet their safety limits at touchdown. The maneuver time ranges from about 5 seconds to 15 seconds, depending on the altitude at which the engine failure occurs.

The effect of engine-failure altitude on the variation of rotor speed is also interesting. For higher engine-failure altitudes, the helicopter can build up airspeed to reduce the power requirement. This permits the rotor speed to increase, after the initial reduction, to replenish the rotational energy in the rotor. This energy is then used

toward the end of the RTO transition flight to cushion the landing. For lower failure altitudes, the helicopter does not have enough altitude range to develop sufficient airspeed for any significant reduction in power required; the rotor speed therefore has to stay at the lower limit to reduce profile power. The thrust coefficient increases gradually until at the end of the transition flight where it decreases, and the rotor speed increases owing to the ground effect. In reality, however, the pilot would likely increase collective pitch in the final seconds before landing, deleting the rotor speed below its calculated value.

Ground effect plays an important role in low speed landing, especially for helicopters with large rotors such as the study helicopter. In fact, calculations of the optimal RTO trajectories are also made without including the ground effect. Results indicate that there is no feasible solution for gross weight of 16,000 lb; a much lower weight has to be used. Therefore, one should consider the presence of ground effect in estimating the maximum payload capability. For VTOL operations from a ground-level confined heliport, ground effect is usually present. On building-top helipads, however, the ground effect is not always as pronounced, depending on the wind conditions. For consistency, all optimal trajectories of RTO and CL in this paper are computed with ground effect included.

Figure 7 shows the effect of helicopter gross weight on the optimal RTO trajectories for P_{OEI} = 1656 hp, V_0 = 5 kt, h_0 = 40 ft, γ_0 = 150°, and with several gross weight values ranging from 15,000 to 16,300 lb. Examinations of rotor-speed time histories in these optimal RTO solutions reveal the gross weight capability of the helicopter for a given OEI power level. For a larger gross weight, the rotor speed stays at the lower limit for a longer portion of the flight, and the final rotor speed is lower. Also, both the airspeed and descent rate reach higher peak values during the flight. No feasible solutions can be obtained if the gross weight is increased further. It was found that the maximum gross weight is defined by a rotor speed history that stays at the lower limit to the end of RTO transition flight.

Investigations were also made using higher OEI power levels and formulating the problem with an alternative performance index to equation (30) to minimize touchdown speeds with a constraint on touchdown point location. As expected, the results indicate that a larger limit of vertical descent rate or horizontal velocity component at touchdown allows the helicopter to carry more payload. However, the most effective way of increasing gross weight capability is by increasing the OEI contingency power available.

B. STOL– *Minimum Runway Problem*– Optimal trajectories that minimize the runway length required (eq. (34)) are shown in figure 8 for the OEI initial conditions of h_0 = 20 ft, γ_0 = 6°, and V_0 = 60 ft/sec. The safe touchdown vertical and horizontal speed limits are 5 ft/sec and 40 ft/sec, respectively, and the gross weight ranges from 18,500 to 19,500 lb. The most interesting feature of the minimum runway RTO is that the optimal trajectories are relatively insensitive to the variation in gross weight. This general characteristic was also observed previously in the flight test with the S76B helicopter reported in reference 11.

Upon an engine failure, the thrust coefficient is decreased to reduce the power required; and at the same time, the thrust vector is tilted backward to the specified maximum limit of 10° to slow down the helicopter in the horizontal direction. After an initial droop in the rotor speed due to the OEI power transient, the rotor speed peaks to reach near its upper limit. As the helicopter approaches the ground, the rotor rotational energy is utilized, through an increase in the thrust coefficient, to arrest the sink rate to meet the safe touchdown speed limits. For the cases shown with initial altitude of 20 ft, the maneuver time is on the order of 4 sec, slightly shorter for a lighter weight configuration. The corresponding minimum airborne runway-length required in a rejected takeoff is on the order of 200 ft (a total runway length of 324 ft including the ground run). The rejected takeoff length increases as the initial altitude (at which an engine failure occurs) increases as discussed in reference 13.

Notice that the gross weight capability for STOL RTO transition flight is considerably higher than the maximum weight in a steady OEI climb shown in table 1. Therefore, the gross weight capability in STOL operations is determined by the CTO segment of the flight, rather than the RTO segment. Because of a much lower speed region in which the VTOL RTO segment operates, compared with its STOL counterpart, the attendant higher power required dictates a considerably lower gross weight capability for the VTOL operation. This can be seen in figures 7 and 8. In fact, in contrast to the STOL case, it is the RTO segment of the flight, not the CTO, which limits the gross weight capability in VTOL operations, as will be discussed subsequently in the paper.

Maximum Takeoff Weight in STOL RTO– Numerical optimization to maximize the RTO gross weight using the performance index of equation (35) was conducted (ref. 13). Extensive numerical runs using a range of h_0, V_0, and γ_0 indicated that the maximum RTO weights are between 21,000–23,000 lb. Therefore, the maximum takeoff weight in a Category-A runway (or STOL) takeoff is determined by continued takeoff and climbout (table 1).

5.4 Continued Takeoff Flight

A. VTOL– Two optimization problems are investigated for CTO transition flight: (1) minimization of the runway length (eq. (34)), and the minimization of the maximum altitude loss (eq. (42b)). The main characteristics of the results are depicted in figures 9 and 10.

Figure 9 compares the optimal trajectories for the above two different performance indices. The flight conditions are W = 16,572 lb, V_0 = 2 ft/sec, γ_0 = 90, and U_2 = 46 ft/sec, with three values of the initial altitude, h_0, at 100, 120, and 140 ft. For minimizing the maximum altitude drop, the optimal trajectories have the identical shape for all three different altitudes at which an engine failure occurs. The control strategy is to rapidly tilt the thrust vector forward to its 10° limit to increase the forward speed, and to increase the collective (or thrust coefficient) to decrease the rotor speed down to its lower limit, trading all possible rotor rotational energy to gain altitude and airspeed. As the power deficiency diminishes with the increase in airspeed around 22 kt, the thrust vector can be rotated backward, somewhat gradually, to reduce the rate of descent and to initiate a climb.

Optimal trajectories that minimize the runway length behave differently for different initial altitude, as expected. As the initial altitude increases, the tradeoff between the potential energy and the rotor speed, and thus the control strategy for the thrust coefficient, is more apparent. The peak descent rate increases and the rotor speed reaches higher values in the middle of the transition flight. Toward the end of the CTO transition flight, the thrust coefficient is increased more rapidly, thereby using the rotational energy reserve of the rotor to arrest the sink rate and then to meet the climb conditions. The control strategy for the thrust inclination remains essentially the same as that for the case of minimization of the maximum altitude drop when the initial altitude changes, resulting in almost identical behavior in airspeed. For all three initial altitudes, the final altitude reaches the same value at 35 ft. However, there is a slight reduction in both the maneuver time and the horizontal distance from those of minimization of the maximum altitude-loss case. The maneuver time for these CTO transition flights is on the order of 14 sec.

The effect of gross weight on the optimal CTO trajectories generated from the two performance indices is also evaluated, and the results are summarized in figure 10. It illustrates the tradeoff between gross weight and the vertical and horizontal space requirements. The OEI conditions are the same as those shown in figure 9, except that the initial altitude is fixed at 100 ft, with three values of gross weight set at 15,856, 16,209, and 16,572 lb (with corresponding U_2 = 38.75, 42.25, 45.75 ft/sec). For a lighter weight, the helicopter can minimize the horizontal distance required to achieve the desired steady OEI climb at the expense of a bigger altitude drop, or the altitude drop can be minimized at the expense of requiring a larger horizontal space. As the gross weight increases, the requirement for achieving the desired OEI climb conditions dominates the solution, and the difference between the optimal trajectories generated from the two performance indices becomes smaller and eventually yields identical solutions as the maximum gross weight is reached. Further increase in gross weight capability is possible through the use of a higher OEI power level, a larger initial airspeed, or a higher initial altitude and thus a larger altitude drop range. Similarly, a lower permissible altitude to clear in a CTO, e.g., the 15 ft recently recommended by the JAA instead of the 35 ft used in this paper to meet the FAA rules, should increase somewhat the gross weight capability, as far as CTO is concerned.

Note that the above results are obtained using the initial flightpath angle, γ_0 = 90° starting from the added small vertical climb segment near the TDP in the backup takeoff procedure (see fig. 2(a)). Without the addition of this vertical segment, the initial condition for the glideslope would be γ_0 = 150°. If this initial condition is used, optimal CTO trajectories will start with a rearward motion, similar to those shown in figures 6 and 7. The pilot usually prefers to fly forward immediately following an engine failure in the CTO transition flight, thus a brief vertical climb segment around the TDP is included in the nominal AEO takeoff path. When γ_0 = 150° is used, the above conclusions are still valid, since the initial flightpath angle does not have significant effect on the CTO paths at low speed.

B. STOL–

Minimum Runway-Length Problem: Extensive trajectory optimization runs were made to investigate the effects of initial states, V_0, h_0, γ_0, and gross weight. These represent the energy state and the power-required level at the moment when an engine failure occurs. Figure 11 shows the effect of the initial airspeed on the optimal CTO trajectories that minimize the runway length (eq. (34)) for h_0 = 20 ft, γ_0 = 6°, Ω_0 = 100%, with U_2 = 70 ft/sec and W = 19,123 lb (see table 1). Upon an engine failure, the optimal control strategy is to rapidly tilt the thrust vector forward about 5° to initiate an acceleration, and at the same time gradually increase the thrust coefficient to reduce the rotor RPM to its lower limit, hence reducing the power required to match the available OEI power. In all but the largest initial-airspeed case, which has a higher associated initial energy level, the rotor speed stays at the lower limit for the entire CTO transition flight. As the airspeed increases to within about

3 to 4 ft/sec of the desired final airspeed, the thrust vector is gradually rotated back to initiate a climbout and to meet the desired final conditions. The maneuver time for the entire CTO transition flight lasts for about 7 to 12 sec, and the horizontal distance ranges from about 480 to 840 ft, with the lowest initial-airspeed case taking the longest time and covering the longest distance.

Thus, for a given initial airspeed, V_0, the higher the value of V_{TOSS}, the longer the runway length is required for the CTO transition flight, although a higher speed provides a higher gross weight capability in steady OEI climbout (see table 1). To determine a suitable value of V_{TOSS} for a given value of V_0, numerical experiments were conducted by varying their differences with values ranging from 5 to 20 ft/sec and with various initial conditions. Results show that a value of about 10 to 15 ft/sec provides a good compromise between the required runway length and the gross weight capability. Figure 12 shows a sample set of results using the initial conditions of V_0 = 50 ft/sec, h_0 = 20 ft, and γ_0 = 5°. The suitable range of $\Delta V = V_{TOSS} - V_0$ = 10 to 15 ft/sec, thus determined, appears to be consistent with the flight manual instructions of the Super Puma (ref. 40). Based on flight test results of the S76-B, reference 11 also suggested that a 10-kt difference between V_{TOSS} and V_0 is appropriate for achieving balanced field length.

Thus, an alternative way of minimizing the runway length can be formulated with a fixed value of $V_{TOSS} - V_0$, such as $V_{TOSS} = V_0 + 15$ ft/sec, and minimizing the runway length for various weights. This approach offers consistency since the pilot does not have to adjust V_{TOSS} when the takeoff weight changes, as is required in the preceding formulation. Results from this alternative formulation are discussed in reference 13.

Maximum Takeoff Weight for CTO: The maximum takeoff weight problem to maximize the performance index (eq. (35)) subject to the specified length (eq. (43)) turns out to be a dual of the minimum runway problem for a given takeoff weight discussed above. The specified takeoff weight in the minimum runway-length problem is, in fact, the same as the solution to the maximum weight problem if the minimum runway length obtained from the first problem is specified for the second problem. Numerical solution of the optimal trajectories from the two problems was found to be almost identical in reference 13.

As the specified runway length decreases, the maximum weight attainable for the OEI CTO transition flight also decreases. As a result, the maximum takeoff weight in CTO is determined by the steady OEI climb requirements if the runway length is sufficient, and is otherwise determined by the available runway length.

5.5 Balked Landing

Regulations require that a balked landing must be possible for an engine failure occurring at and prior to the landing decision point along the nominal AEO landing path. The terminal conditions for a BL transition flight are the same as for the CTO transition flight described earlier, except for the use of the balked landing safety speed, V_{BLSS}, instead of the takeoff safety speed, V_{TOSS}. However, the two safety speeds are often selected to be the same.

A. VTOL– The results of balked landing optimal trajectories are generally similar to those of continued takeoff. However, balked landing results have some unique characteristics. Due to a higher initial airspeed and a lower power required in a descent, a balked landing for an engine failure occurring at a higher altitude provides a larger gross weight capability compared with its continued takeoff counterpart. Also, since the airspeed decreases along the nominal AEO landing path, the maximum gross weight possible in a balked landing reduces significantly as the altitude decreases.

B. STOL– The optimal trajectories for the STOL balked landing transition flights are again generally similar to those of STOL continued takeoff. Figure 13 shows the effect of the initial airspeed on the minimum runway-length optimal BL trajectories for W = 19,123 lb, U_2 = 70 ft/sec, with the initial OEI flight conditions of h_0 = 125 ft and γ_0 = –3°. Upon an engine failure, the optimal control strategy is to rapidly tilt the thrust vector forward, some 7° to 9° depending on the initial airspeed, to accelerate the aircraft and reduce the power required. At the same time, the thrust coefficient is increased to reduce the rotor RPM to its lower limit, further reducing the power required to accommodate the power loss. As the airspeed increases, and thus the power required decreases, the thrust vector is rotated back to initiate a climbout and to meet the specified final conditions. The transitional flight time is on the order of 8 sec. The horizontal distance covered is about 530 ft.

This optimal control strategy is very similar to that used in the CTO case shown in figure 11. However, because of the higher initial altitude and the attendant higher potential energy for the BL case, the rotor rotational energy is partially replenished during the ensuing transition flight, and is then used to assist the climb. At the end of the transition flight the rotor speed reaches the lower limit, and the power required matches the power available, thus establishing the desired steady OEI climb.

5.6 Continued Landing Flight

A. VTOL– Optimal trajectories that minimize the heliport size requirement (eq. (30)) are calculated for OEI-CL transition flight with various initial conditions. Results show some features are significantly different from those of the RTO counterpart in VTOL operations, which are generated from the same performance index as discussed previously.

Figure 14 shows a set of sample results with W = 16,000 lb, P_{OEI} = 1656 hp, and γ_0 = –6°. Because of a higher initial velocity associated with a higher initial altitude along the AEO landing path, the optimal OEI-CL trajectories are considerably different for an engine failure occurring at different altitudes. This is a result of the difference not only in the initial energy state (such as the case of RTO shown in fig. 6), but also in the power required at the moment when an engine loses its power. For example, at h_0 = 100 ft with the associated initial airspeed, V_0 = 59 ft/sec (or 35 kt), the power required on the AEO landing path with a 6° glideslope is less than the OEI power available for the gross weight of 16,000 lb. Since the OEI available power is assumed to automatically increase to its maximum after an engine failure, the helicopter experiences a power excess and has to increase its power required to match the power available. As a result, the rotor speed increases. As shown in the figure, a similar situation also occurs for the initial conditions of h_0 = 80 ft and V_0 = 50.6 ft/sec. As the initial altitude and airspeed decrease along the nominal AEO landing path, the power required increases, and the optimal OEI CL trajectories are gradually characterized by a power deficiency, resembling those of the RTO shown in figure 6. Thus, for the lower altitude and lower airspeed cases, the rotor speed reduces to and stays at its lower limit until near touchdown, where it increases due to the ground effect. In actuality, however, the pilot would likely increase the collective in the final seconds before touchdown and reduce the rotor speed to below the calculated value.

The maximum gross weight is limited by continued landing at lower initial altitudes along the nominal AEO landing path that was considered. In fact, no feasible solutions can be obtained when the gross weight is increased to 16,500 lb or higher for continued landing starting at h_0 = 25 ft and V_0 = 0. Gross weight capability increases as the initial altitude and the associated initial airspeed increase. This limitation is consistent with the typical H-V diagram of a helicopter.

B. STOL– The landing decision point (LDP) is usually chosen such that its necessary energy level, together with its limited decreasing rate, permits a successful OEI-BL flight. As a result, the LDP altitude is typically 100 ft or higher, airspeed at LDP is usually a moderate 40 kt or so, and rate of descent is limited to about 400 fpm or lower. Because of the higher initial altitude together with a lower power required in a descent, the OEI-CL trajectories that minimize the runway length (eq. (34)) have characteristics distinctively different from its RTO counterpart.

Figure 15 shows a family of minimum runway OEI-CL trajectories calculated for a range of gross weights with the initial conditions, h_0 = 125 ft, γ_0 = –3°, and V_0 = 55 ft/sec. Compared with its RTO counterpart as shown in figure 8, it is seen that, while the control strategy for the thrust coefficient and thus the resulting descent rate and rotor speed are generally similar, the control strategy for the thrust inclination and the resulting horizontal speed response are considerably different. Because of the lower power required in a descent together with a higher energy level at the moment when an engine failure occurs in the case of OEI CL, there is more exchange taking place among the helicopter potential, kinetic and rotor rotational energy sources. This is reflected in the control reversals, especially in the thrust inclination. Unlike the RTO case, the change in gross weight does alter significantly the time histories of the control inclination and the attendant speed. The helicopter has to maintain a higher airspeed during the transition flight to carry a heavier load. For the conditions shown, the CL transition flight time is slightly over 8 sec, depending on the gross weight, and is about twice as long as that of the RTO transition flight. It also covers a longer horizontal distance, some 340 ft, and is about 70% longer than that required for the RTO.

5.7 Conditions of the Decision Points

Definition of specific conditions of the takeoff decision point and landing decision point requires a comprehensive evaluation of the effects of weight, altitude, temperature and wind conditions using a high-fidelity mathematical model of the helicopter. While the augmented point mass model used in this paper falls short of meeting the requirements, it is useful, nevertheless, for exploring the basic tradeoffs in Category-A terminal area operations. Two concepts related to the choice of the takeoff decision point for STOL and VTOL Category-A operations are discussed in the following paragraphs.

Takeoff decision point – STOL– By combining the results of CTO and RTO, some insights into the choice of the takeoff decision point can be obtained. Figure 16 shows such a combined plot, indicating the minimum runway field lengths required for both the RTO and CTO for the flight conditions at V_0 = 50 ft/sec, W = 18,610 lb, and γ_0 = 5°, 7°, and 9°. The total runway lengths

required are calculated by combining the airborne segments (the AEO segment and the OEI transition flight segment) and ground run in the case of RTO.

$$X_{CTO} = \frac{V_0^2}{0.4g} + \frac{h_0 - 5}{\tan\gamma_0} + x_{f\cdot cto} \quad \text{(ft)} \qquad (44)$$

$$X_{RTO} = \frac{V_0^2 + u_{\max}^2}{0.4g} + \frac{h_0 - 5}{\tan\gamma_0} + x_{f\cdot rto} \quad \text{(ft)} \qquad (45)$$

The choice of decision height can now be made with the aid of figure 16. For example, if one opts to use the criterion of balanced field length (BFL), whereby the RTO and CTO require the same runway length, TDP altitude will be 23.5 ft for an initial flightpath angle of 5°. As the initial flightpath angle increases, the TDP altitude and the corresponding BFL decrease. This figure can also be used to determine the best TDP altitude for unbalanced field length, if heliport configurations so dictate.

The choice of the TDP velocity affects both the runway length and the gross weight capability. Since the CTO flight segment determines the maximum takeoff weight capability, a higher TDP velocity results in a higher payload capability. However, this requires a longer runway length.

Balanced-weight concept for TDP altitude– VTOL– For a given OEI power and the specified AEO VTOL flightpath, the gross weight capability is determined by the rejected takeoff and the continued landing flight phases. The maximum gross weight possible in a RTO or a CL is limited by the high power required at low speeds and by the shape of the OEI H-V diagram. To land safely on the helipad, the airspeed has to be low. As discussed earlier, rejected takeoffs are most difficult for engine failures occurring at a certain band of altitudes reflective of the OEI H-V diagram. Once above this critical altitude band, there is no advantage in locating the TDP altitude very high, since it must be possible to achieve a safe RTO at any point up to the TDP. However, from the perspective of the CTO or BL, gross weight capability is increased with the increase in the TDP altitude. Since the takeoff gross weight capability is limited by the lower of the maximum gross weights possible in the RTO or in the CTO, it is proposed to use a “balanced-weight” criterion for determining the TDP altitude. At this altitude, the maximum gross weight in CTO is about the same as that in RTO.

5.8 Real-Time Generation of Optimal Trajectories

As discussed in the preceding section, the optimal control strategies and the associated optimal trajectories are sensitive to the initial conditions. It is a challenge, therefore, to convey these optimal control strategies to assist the pilot, in a timely fashion, to cope with the situation when an engine failure occurs. Due to the large number of states and constraints, numerical solutions usually take a long time, even on a mainframe computer. The capability to provide a reliable real-time generation of optimal trajectories on board the aircraft with limited computing power and memory is extremely challenging.

A technique for real-time generation of *approximate* optimal trajectories has recently been proposed (ref. 20) based on curve-fitting and interpolation. First, the optimal trajectories are solved off-line in a manner similar to that described in this paper. These off-line computed optimal trajectories are then approximated with a Fourier series. Finally, the Fourier coefficients are interpolated with multi-dimensional polynomials of initial conditions (i.e., $h_0, V_0, \gamma_0, \Omega_0$) and the control parameters, W, P_{OEI}. To facilitate this difficult interpolation process, a special scheme was devised to reduce the multi-dimensional fitting problem into several smaller independent problems in a nested fashion. Details are discussed in reference 20.

6. Conclusions

This paper summarizes some key results of a series of trajectory optimization studies conducted to examine basic characteristics of a twin engine helicopter in Category-A, one-engine-inoperative, takeoff and landing operations. Using an eight state, two controls, augmented point-mass model representative of the study helicopter, rejected takeoff, continued takeoff, balked landing, and continued landing are investigated for both vertical takeoff and landing to or from a helipad and short takeoff and landing to or from a clear heliport. For VTOL operations, a linear backup procedure is assumed for normal all-engine-operating takeoff, and a straight-in procedure for normal landing. In rejected takeoff and continued landing, optimal trajectories are calculated to minimize the deviations of the touchdown point from the original takeoff point, subject to safe touchdown speed limits. For continued takeoff and balked landing, two performance indices are considered: one minimizes the horizontal distance, and the other minimizes the maximum altitude drop. Both are subject to terminal constraints corresponding to the steady OEI climb required by the FAA regulations. In STOL operations, which use a typical normal AEO takeoff and landing procedure, two trajectory optimization problems are formulated for OEI transitional flight: one to minimize the runway length requirements and another to maximize the takeoff weight. Both are subject to appropriately specified terminal conditions. The major results from these extensive optimization studies show that:

1. The rejected takeoff and continued landing flight phases determine the maximum gross weight capability for VTOL Category-A operations. For STOL operations, it is the continued takeoff and balked landing flight phases that limit the gross weight capability.

2. In an OEI transitional flight, the optimal control strategies are such that they maneuver the helicopter to match the power required to the level of the OEI contingency power available, along the way trading among the helicopter's potential, kinetic, and rotor rotational energy sources.

3. For a VTOL rejected takeoff, the typical optimal control strategy after an engine failure is to tilt the thrust vector forward initially to increase the airspeed and to increase the thrust coefficient to reduce the rotor speed, thereby reducing the power required. Subsequently, the thrust vector is tilted backward to arrest the sink rate and reduce airspeed to satisfy the safe touchdown speeds. In contrast, for a STOL RTO transitional flight, the thrust vector is tilted backward to its specified limit to reduce the horizontal speed, and at the same time the collective is reduced to increase the rotor speed. Collective is then increased to arrest the sink rate and to make use of the rotor rotational energy for cushioning the landing. The STOL RTO trajectories are relatively insensitive to gross weight variation. The RTO transitional flight is typically very short, on the order of only 4 sec.

4. Upon an engine failure in a VTOL continued takeoff, the optimal control strategy is to tilt the thrust vector forward to its specified limit to accelerate the helicopter toward V_{TOSS}, and to increase the collective to reduce the rotor speed to its lower limit, trading the rotor rotational energy to gain airspeed and altitude. Depending on how the collective is used and the rotor speed is managed, one can trade off the horizontal distance required with the maximum allowable altitude drop. Optimal control strategies for STOL CTO are generally similar to those for the VTOL counterpart; however, because of a higher initial airspeed, the thrust vector is tilted forward less than in the VTOL CTO case.

5. The balked landing and continued landing are generally similar to CTO and RTO, respectively. However, because of the lower power required associated with a descent, coupled with a higher energy level at the moment when an engine failure occurs, more energy exchange takes place for a typical BL or CL, reflecting in more control reversals, especially in the thrust inclination.

6. A balanced field length concept can be used for determining the takeoff-decision-point altitude for STOL operations. Similarly, a balanced-weight concept can serve as a means of determining the TDP altitude for VTOL operations. These concepts are described in section 5.7.

7. The differential between V_{TOSS} and the TDP airspeed of 10 to 15 ft/sec is shown to be a desirable range from the optimization studies, which is consistent with the flight test results of the S76B and flight manual of the Super Puma.

8. Ground effect is found to be important in trajectory optimization for VTOL RTO and CL transitional flight phases, especially in the determination of the maximum gross weight capability.

References

1. FAA Advisory Circular, Certification of Transport Category Rotorcraft, AC-29A, 1987.
2. Draft JAR 29 Subpart B Performance Requirements, NPA 29-2, Preliminary Issue 1, undated.
3. Lande, K.: New Offshore Helicopter Rig Takeoff and Landing Procedures. Proceedings of Society of Experimental Test Pilots 33rd Symposium, Sept. 1989, pp. 179–204.
4. Stevens, J.M.G.F. and Vodegel, H.J.G.C.: S-76B Certification for Vertical Take- Off and Landing Operations from Confined Areas. 16th European Rotorcraft Forum, Glasgow, UK, Sept. 1990.
5. Vodegel, H.J.G.C. and Stevens, J.M.G.F.: A Computer Program for the Certification of Helicopter Vertical Takeoff and Landing Operations and an Application to the S-76B Helicopter. Proc. AHS Annual Forum, May 1991, pp. 721–731.
6. Goldenberg, J., Meslin, L., Blondino, M., and Williams, D.: Certification of Model 230 Helicopter for Category 'A' Elevated Helipad Operations. Proc. AHS Annual Forum, May 1993, pp. 1497–1505.
7. Wood, T. L., Blondino, M., and Williams, D.: M 230 Helicopter Performance for Category A Elevated Helipad Operation. 19th European Rotorcraft Forum, Cernobbio, Italy, Sept. 1993.
8. Okuno, Y. and Kawachi, K.: Optimal Takeoff of a Helicopter for Category A STOL/VTOL Operations. Journal of Aircraft, Vol. 30, No. 2, March–April, 1993, pp. 235–240.
9. Sharma, V., Zhao, Y., and Chen, R.T.N.: Optimal Sideway Operation of a Category-A Helicopter from an Elevated Helipad. AHS Annual Forum, June 4–6, 1996.
10. Zhao, Y., Jhemi, A. A., and Chen, R.T.N.: Optimal VTOL Operation of a Multiengine Helicopter in the Event of One Engine Failure. AIAA Paper 95-3178, Aug. 1995.
11. Saal, K. W. and Cole, J. L.: Category 'A' Certification of S-76B Featuring Variable CDP and V2 Speeds. J. AHS, July 1990, pp. 12–21.
12. Cerbe, T. and Reichert, G.: Optimization of Helicopter Takeoff and Landing. J. Aircraft, Vol. 26, No. 10, Oct. 1989, pp. 925–931.
13. Zhao, Y. and Chen, R.T.N.: Critical Considerations for Helicopters During Runway Takeoffs. J. Aircraft, Vol. 32, No. 4, July–August 1995, pp. 773–781.
14. Sharma, V.: Optimal Helicopter Operation from a Clear Heliport in the Event of One Engine Failure. Ph.D. Dissertation, Dept. of Aerospace Engr. and Mechanics, University of Minnesota, Nov. 1994.
15. Sharma, V., Zhao, Y., Chen, R.T.N., and Hindson, W. S.: Optimal OEI Clear Heliport Operation of a Multiengine Helicopter. Proc. AHS Annual Forum, May 1995.
16. Schmitz, F. H.: Optimal Takeoff Trajectories of a Heavily Loaded Helicopter. J. Aircraft, Vol. 8, No. 9, Sept. 1971, pp. 717–723.
17. Johnson, W.: Helicopter Optimal Descent and Landing After Power Loss. NASA TM-73244, May 1977.
18. Lee, A. L., Bryson, A. E., and Hindson, W. S.: Optimal Landing of a Helicopter in Autorotation. J. Guidance, Control, and Dynamics, Vol. 11, No. 1, Jan.–Feb. 1988, pp. 7–12.
19. Okuno, Y., Kawachi, K., Azuma, A. and Saito, A.: Analytical Prediction of Height- Velocity Diagram of a Helicopter Using Optimal Control Theory. J. Guidance, Control, and Dynamics, Vol. 14, No.2, Mar.–Apr. 1991, pp. 453–459.
20. Jhemi, A. A., Zhao, Y., and Chen, R.T.N.: Real-Time Generation of Optimal Helicopter Trajectories for Cockpit Display. AIAA Paper 96-0792, AIAA Aerospace Sciences Meeting, Reno, NV, Jan. 1996.
21. Talbot, P. D., Tinling, B. E., Decker, W. A., and Chen, R.T.N.: A Mathematical Model of a Single Main Rotor Helicopter for Piloted Simulation. NASA TM-84281, Sept. 1982.
22. Johnson, W.: Helicopter Theory. Princeton University Press, 1980, pp. 282–283.
23. Gessow A. and Myers, G. C., Jr.: Aerodynamics of the Helicopter, Frederick Ungar Publishing Co., New York, 1952.
24. Stepniewski, W. Z. and Keys, C. N.: Rotary-Wing Aerodynamics, Dover Publications, Inc., 1984.
25. Chen, R.T.N.: A Survey of Nonuniform Inflow Models for Rotorcraft Flight Dynamics and Control Applications. NASA TM-102219, Nov. 1989.

26. Cheeseman, I. C. and Bennett, N. E.: The Effect of the Ground on a Helicopter Rotor in Forward Flight. British R&M, No. 3021, Sept. 1955.

27. Prouty, R. W.: Helicopter Performance, Stability, and Control, Krieger Publishing Co., 1990, p. 698.

28. Curtiss, H. C., Jr., Sun, M., Putman, W. F., and Hanker, E. J.: Rotor Aerodynamics in Ground Effect at Low Advance Ratios. J. AHS, Vol. 29, No. 1, Jan. 1984.

29. Cerbe, T., Reichert, G., and Curtiss, H. C., Jr.: Influence of Ground Effect on Helicopter Takeoff and Landing Performance. Paper No. 70, 14th European Rotorcraft Forum, Milano, Italy, Sept. 20–23, 1988, pp. 70-1 to 70-17.

30. Hirschkron, E., Martin E., and Samanich, N.: Powerplant Design for One Engine Inoperative Operation. Vertiflite, Vol. 30, No.5, July/August 1984, pp. 34–38.

31. Trivier, D. and Bosqui, O.: 30-Second/2-Minute One Engine Inoperative Certification for the AS 332 Super Puma MK II. Proc. 18th European Rotorcraft Forum, Sept. 1992, pp. 129-1 to 129-15.

32. Dept. of the Army: Operator's Manual: UH-60A and EH-60A Helicopters. TM 55-1520-237-10, Jan. 1988.

33. Ballin, M. G. and Dalang-Secretan, M. A.: Validation of the Dynamic Response of a Blade-Element UH-60 Simulation Model in Hovering Flight. J. AHS, Vol. 36, No. 4, Oct. 1991, pp. 77–88.

34. Howlett, J. J.: UH-60A Black Hawk Engineering Simulation Program. Vol. 1, NASA CR-166309, Dec. 1981.

35. Hilbert, K. B.: A Mathematical Model of the UH-60 Helicopter. NASA TM-85890, April 1984.

36. Johnson, C. D.: Optimal Control with Chebyshev Minimax Performance Index. J. Basic Engineering, June 1967, pp. 251–262.

37. Miele, A., Lamoulakis, J. N., Cloutier, J. R., and Tietze, J. L.: Sequential Gradient Restoration Algorithm for Optimal Control Problems with Non-differential Constraints. J. of Optimization Theory and Applications, Vol. 13, No. 2, Feb. 1974, pp. 218–255.

38. Zhao, Y.: Several Trajectory Optimization Problems. Dept. of Aerospace Engineering and Mechanics, University of Minnesota, 1989.

39. Jacobson, D. H. and Lele, M. M.: A Transformation Technique for Optimal Control Problems with a State Variable Inequality Constraint. IEEE Trans. Automatic Control, Vol. AC-14, No. 5, Oct. 1969, pp. 457–464.

40. Super Puma MK2 Supplement for Category A Operations. Undated Flight Manual.

Appendix – Helicopter Parameters Used for Optimization Studies

The study helicopter has a maximum takeoff weight of 22,000 lb and a maximum takeoff power of 3,086 shp. Other related parameters are: R = 26.83 ft, σ = 0.0821, Ω_0 = 27 rad/sec, $C_{T_{\max}}$ = 0.01846, and I_R = 7,060 slug ft^2. Parameter values used in the optimization studies are: f_e = 30 ft^2, ρ = 0.002377 slug/ft^2, g = 32.2 ft/sec^2, c_d = 0.012, η = 0.9, K_{ind} = 1.15, $\beta_{\max}$ = 10°, $\beta_{\min}$ = –10°, $\overline{\Omega}_{\max}$ = 107%, $\overline{\Omega}_{\min}$ = 91%, $w_{\max}$ = 5 ft/sec, $u_{\max}$ = 15 ft/sec for VTOL and 40 ft/sec for STOL, τ_p = 1.5 sec, P_a = 47.3 hp, $P_{OEI,110\%}$ = 1656 hp, and $P_{OEI,105\%}$ = 1580 hp. The thrust constraints used in the optimizations are: $C_{T_{\min}}$ = 0.002 and $C_{T_{\max}}$ = 0.025; these limits are not encountered in the optimization process.

Table 1. Maximum weight in steady OEI climb (P_{OEI} = 1656 hp; SLS; climb rate = 100 fpm; 100% RPM)

U_2, fps	W, lb
55	17,554
60	18,086
65	18,610
70	19,123
75	19,621
80	20,101
85	20,561
90	20,999
95	21,413
100	21,802

(a)

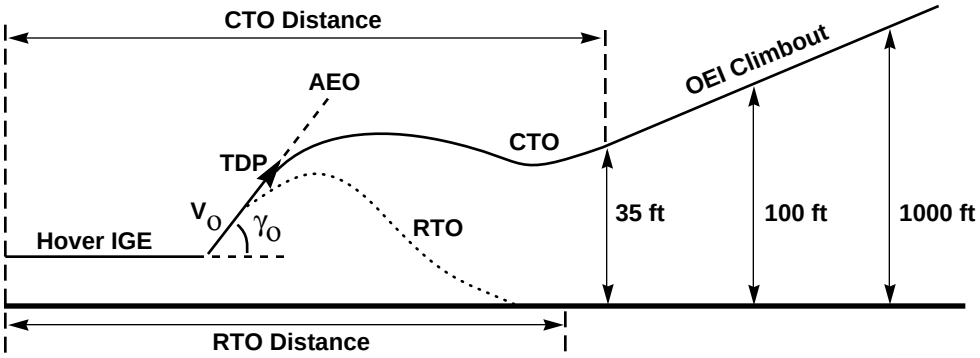

FAA OEI STOL Takeoff Requirements				
Rating	**AEO TOP***	**2.5 min**	**2.5 min**	**30 min**
Airspeed	**0 → V_{TDP}**	**V_{TDP} → V_{TOSS}**	**V_{TOSS}**	**V_Y**
R/C, fpm	**N/A**	**N/A**	**100**	**150**
Rotor rpm	**N/A**	**N/A**	**N/A**	**100%**

***TOP = Takeoff Power**

(b)

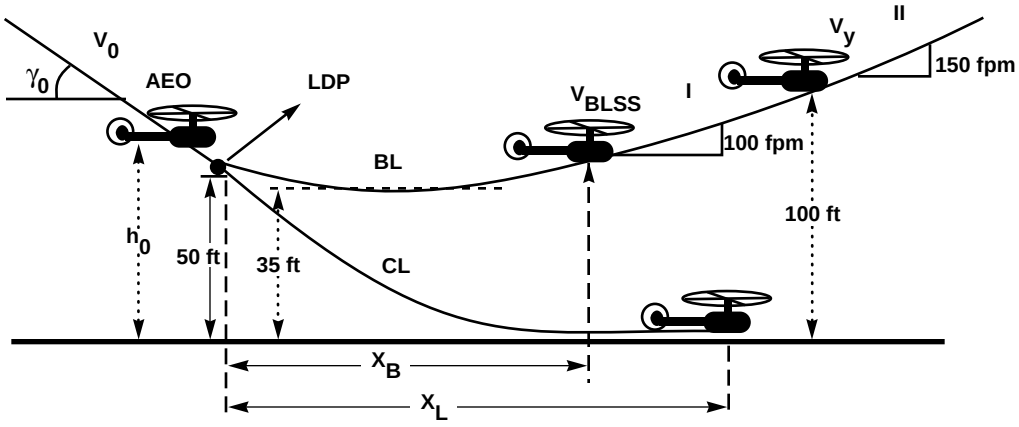

Figure 1. Category-A clear heliport (or STOL) operation: (a) takeoff, (b) landing.

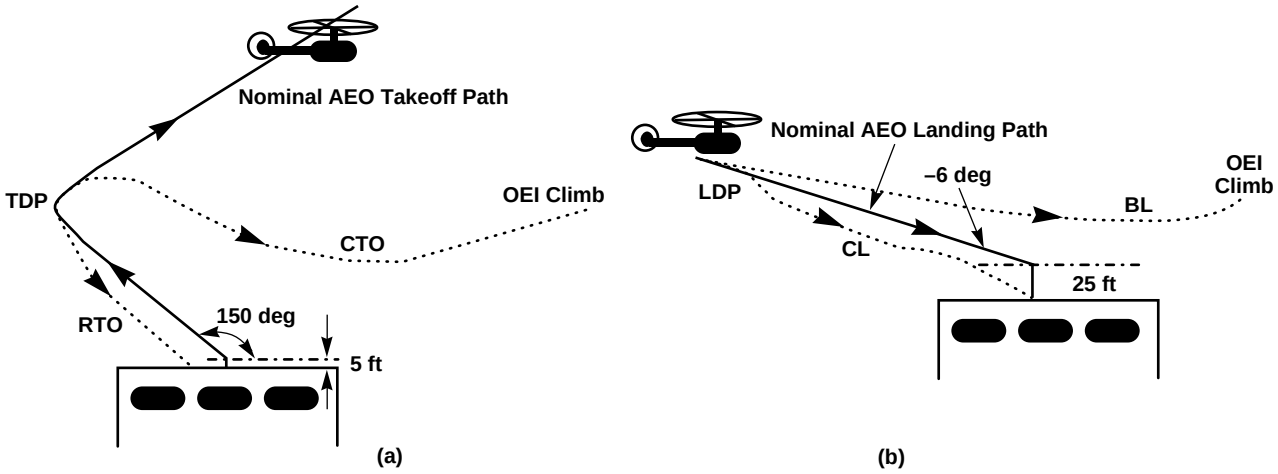

Figure 2. Example VTOL Category-A operation: (a) backup takeoff, (b) landing.

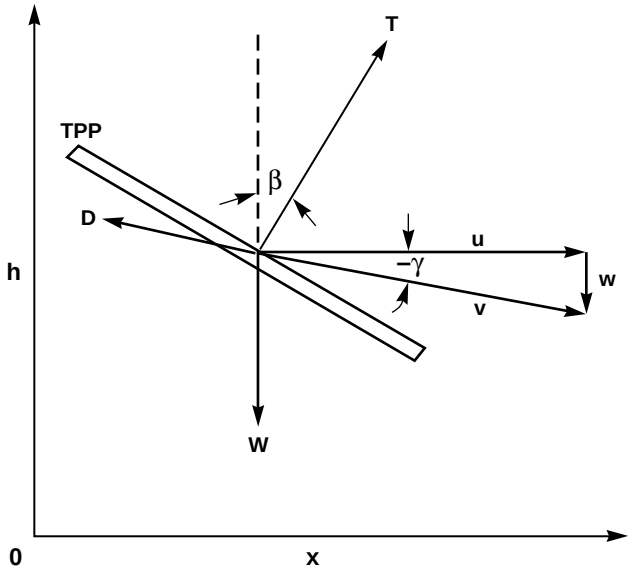

Figure 3. Point-mass helicopter model.

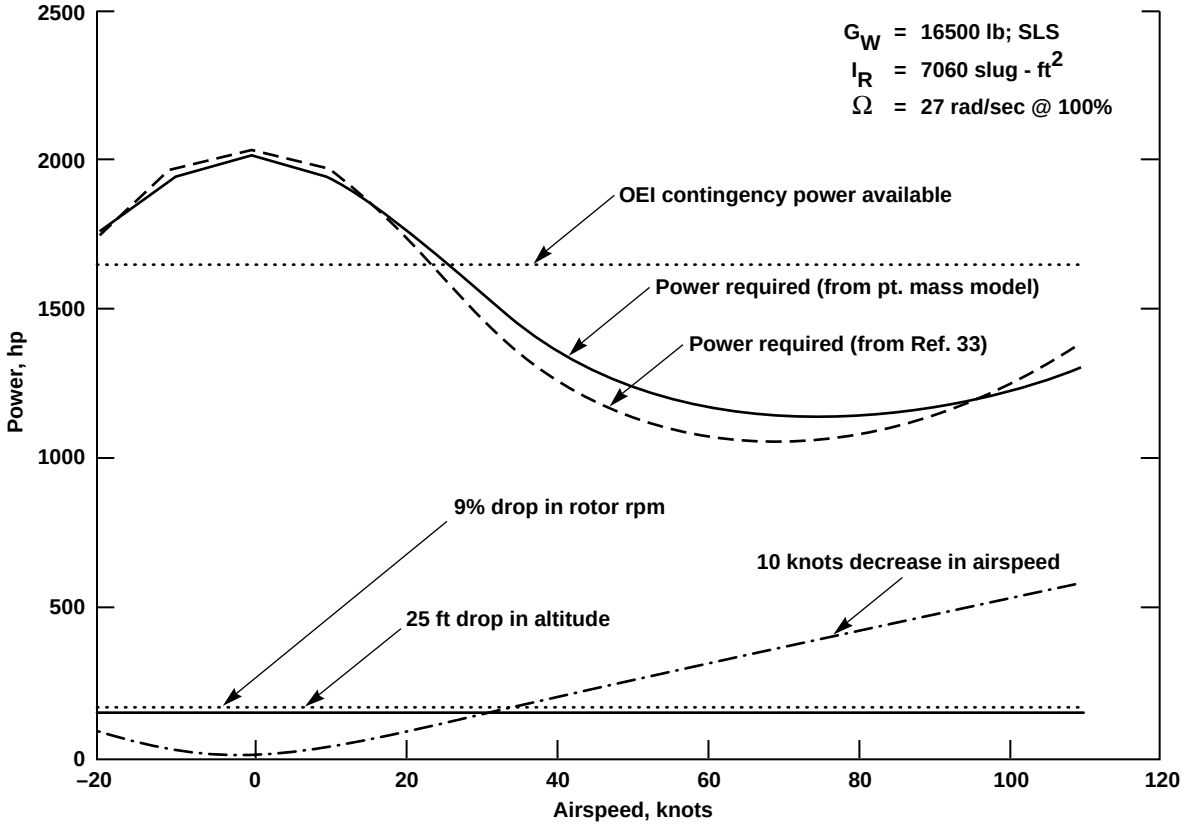

Figure 4. Power components available for tradeoff in OEI maneuver – 5-sec average.

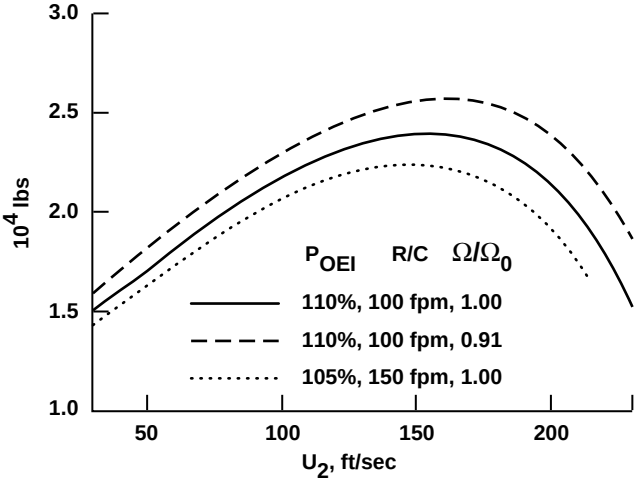

Figure 5. Maximum weight in steady OEI climb.

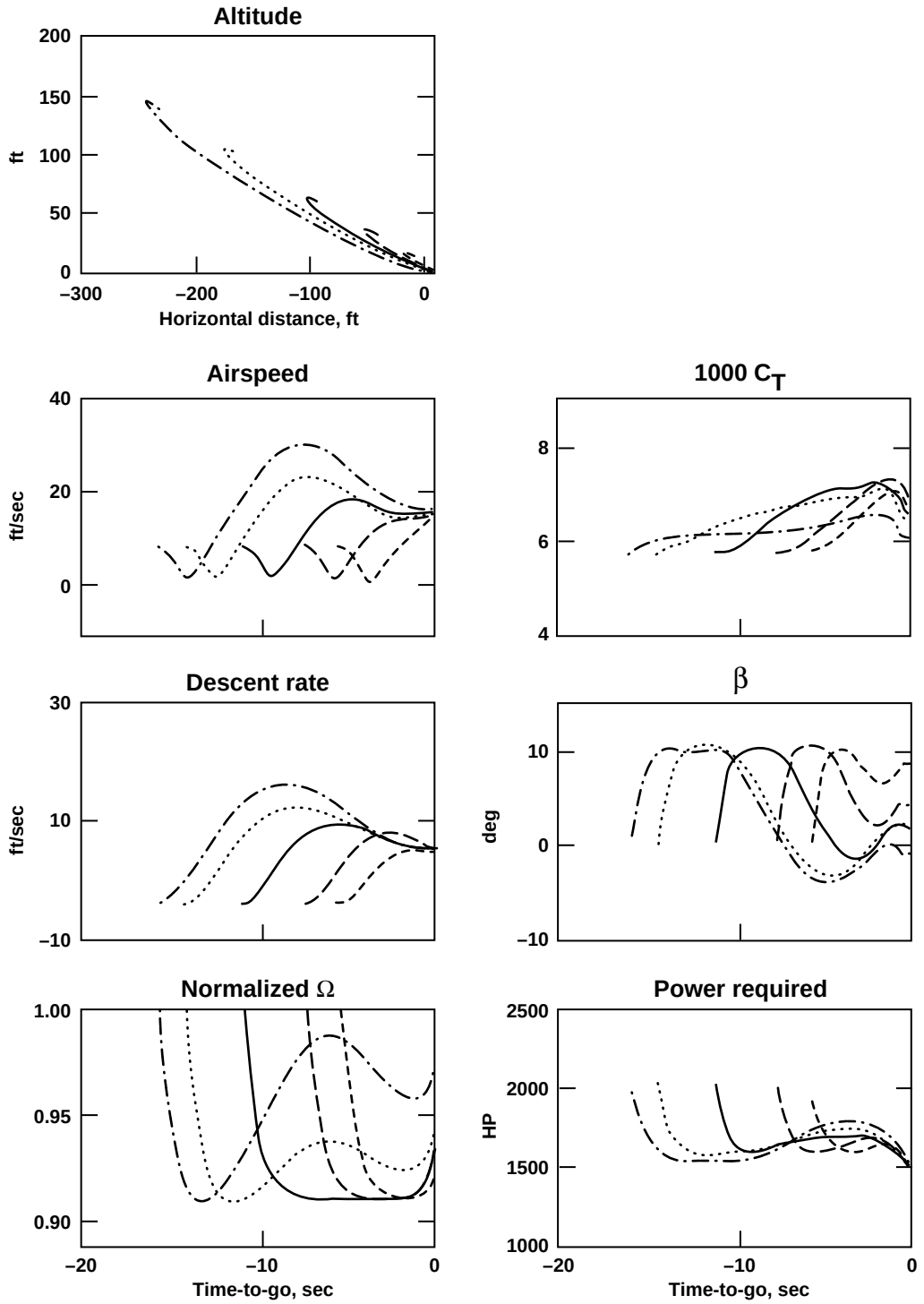

Figure 6. Optimal VTOL- RTO trajectories: W = 16,000 lb, P_{OEI} = 1656 hp, V_0 = 8.4 ft/sec, and γ_0 = 150°.

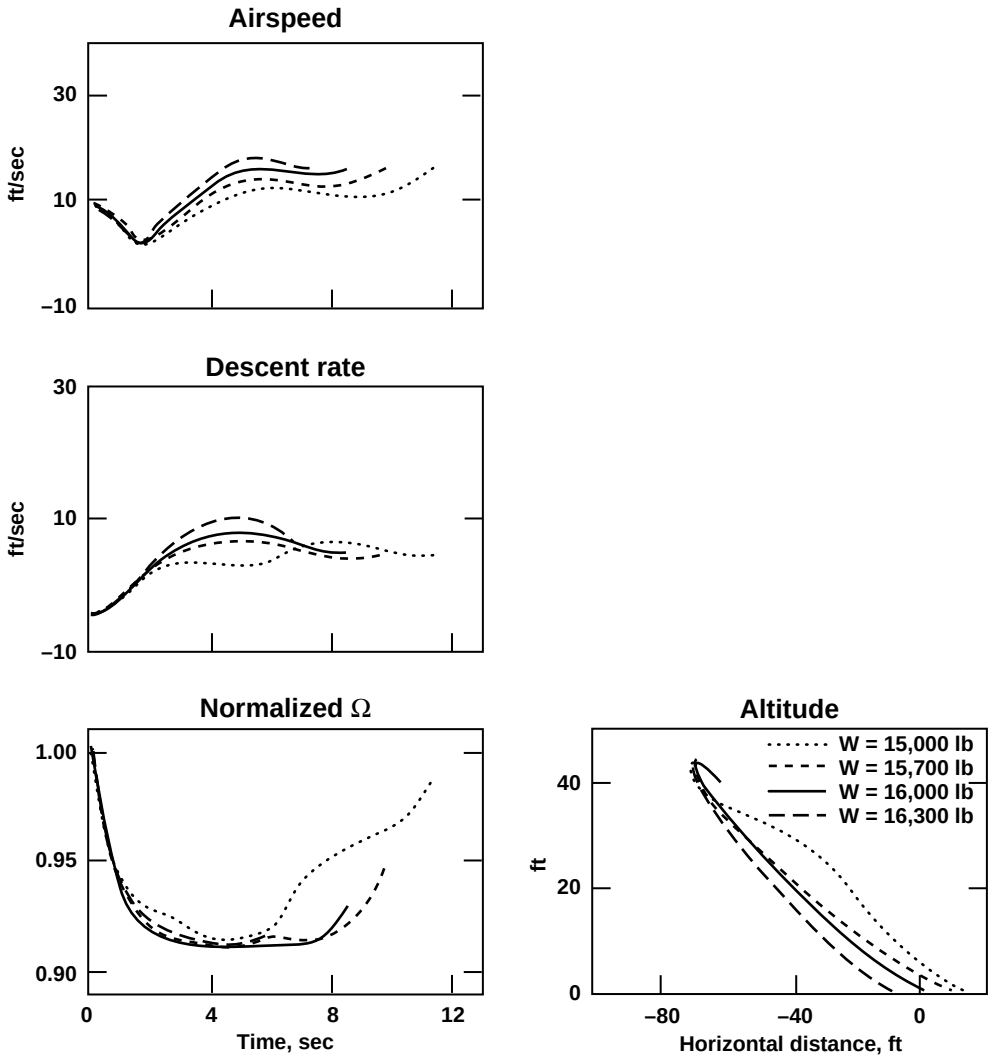

Figure 7. Effect of helicopter gross weight on optimal VTOL- RTO trajectories: P_{OEI} *= 1656 hp,* h_0 *= 40 ft,* V_0 *= 8.4 ft/sec, and* γ_0 *= 150°.*

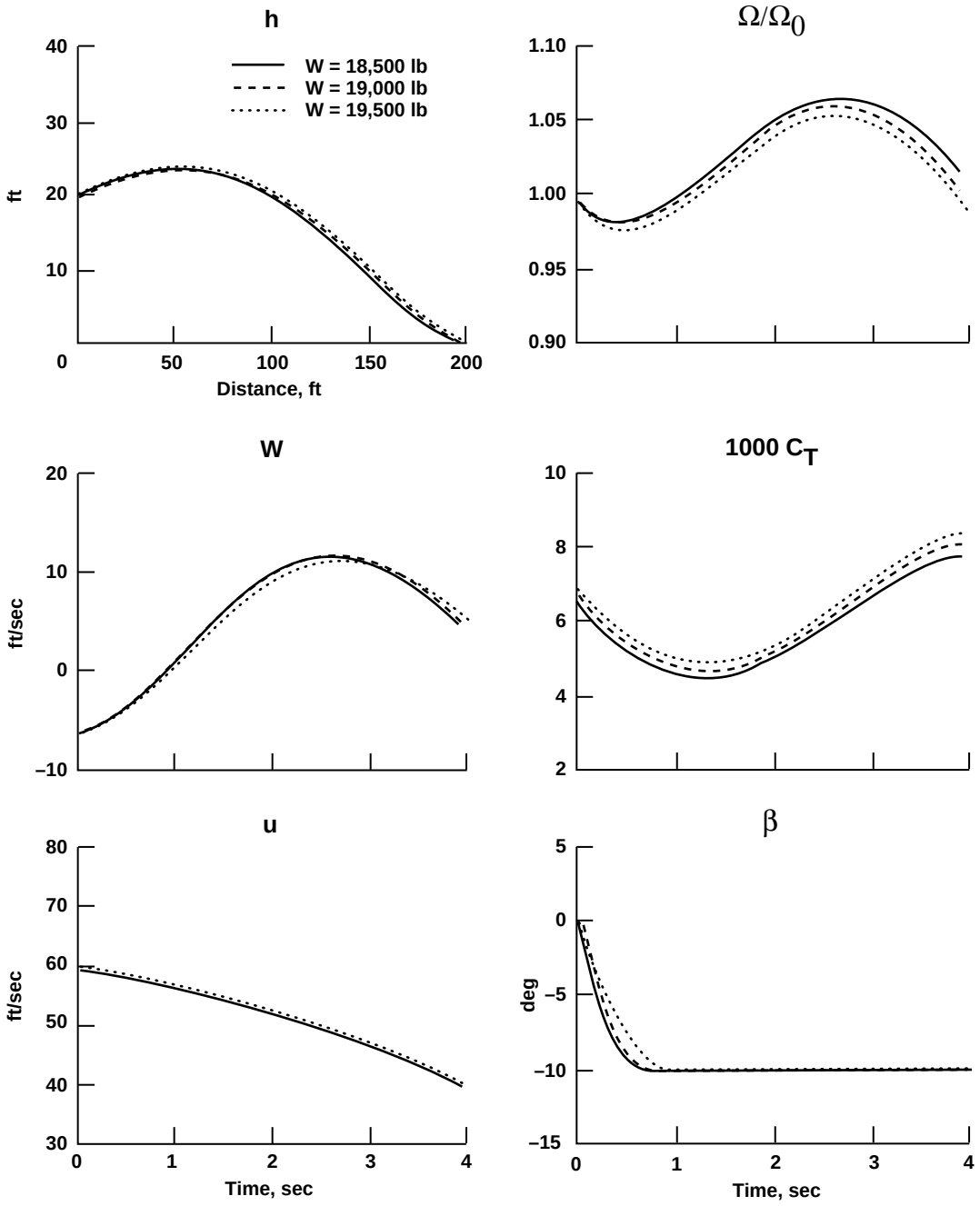

Figure 8. Effect of helicopter gross weight on optimal STOL - RTO trajectories: P_{OEI} = 1656 hp, h_0 = 20 ft, V_0 = 60 ft/sec, and γ_0 = 6°.

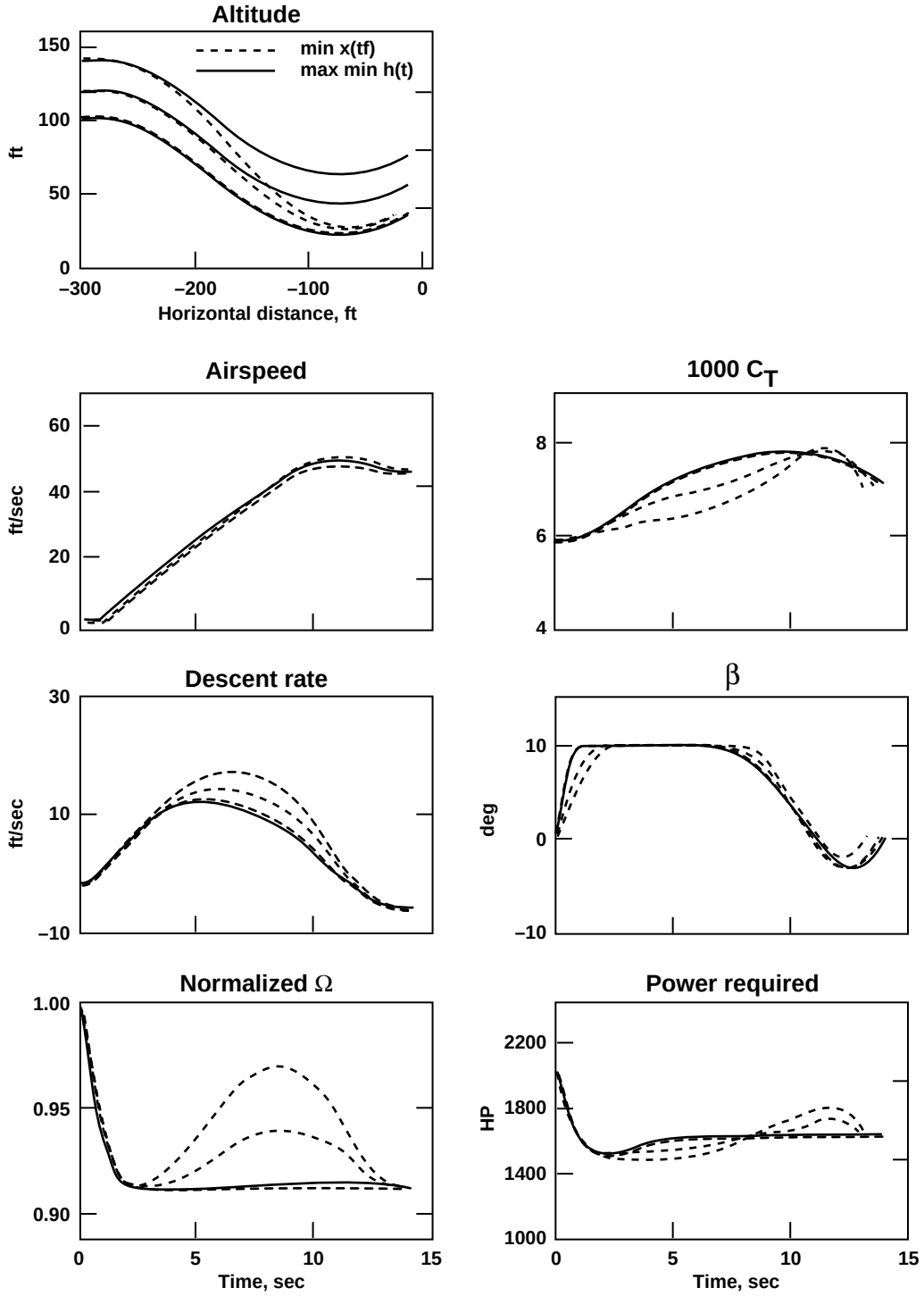

Figure 9. Optimal VTOL- CTO trajectories: W = 16,572 lb, U_2 = 46 ft/sec, P_{OEI} = 1656 hp, γ_0 = 90°, and V_0 = 2 ft/sec.

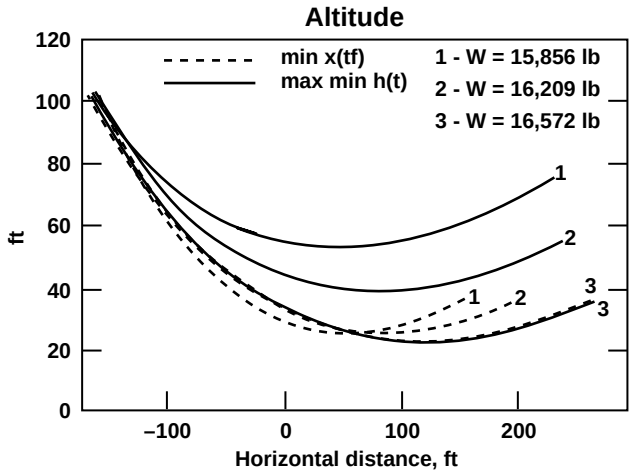

Figure 10. Effect of gross weight and performance indices on VTOL- CTO trajectories: P_{OEI} *= 1656 hp,* h_0 *= 100 ft,* V_0 *= 2 ft/sec, and* γ_0 *= 90°.*

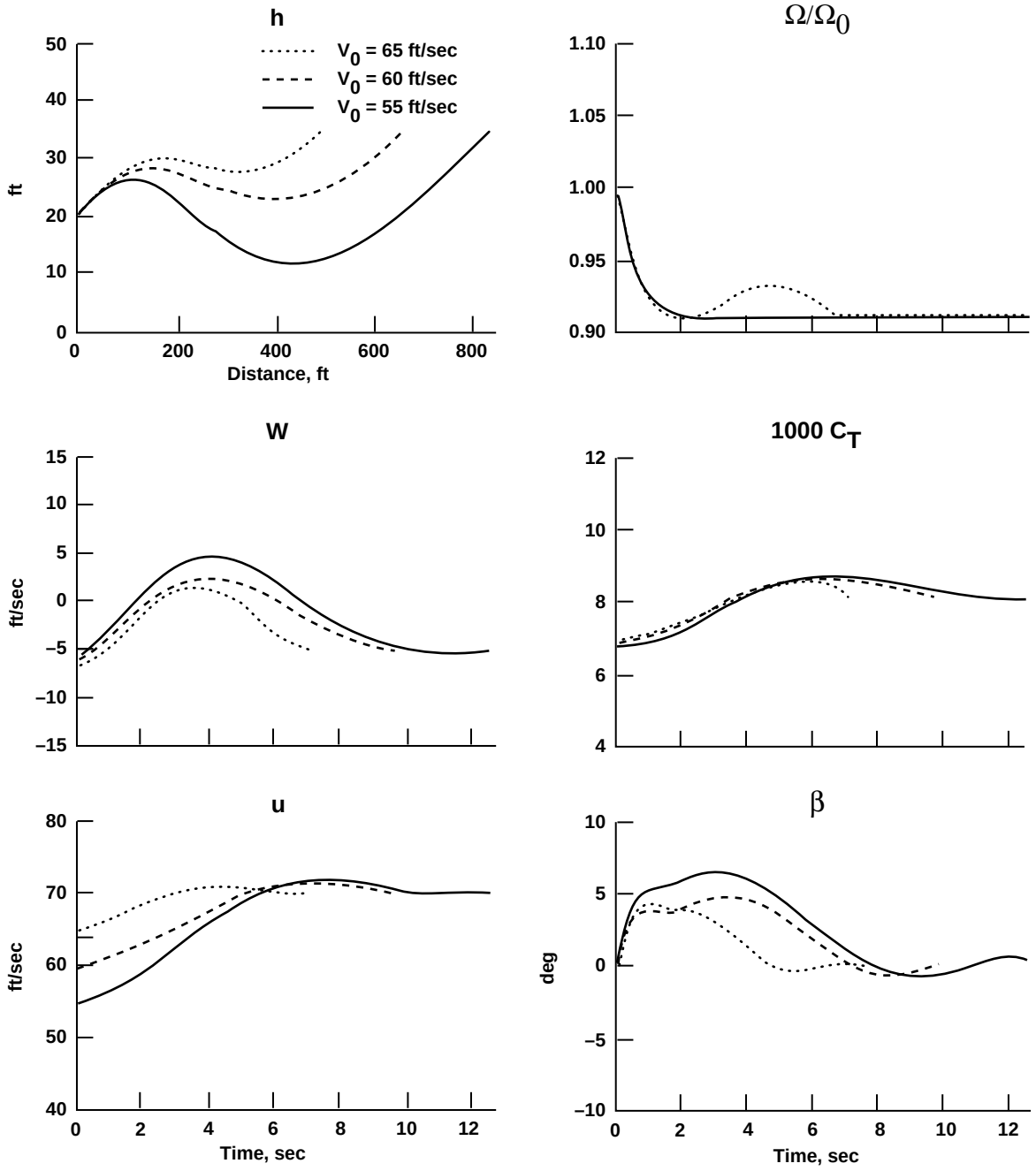

Figure 11. Minimum runway STOL- CTO with different initial airspeeds: h_0 = 20 ft, γ_0 = 6°, W = 19,123 lb, and U_2 = 70 ft/sec.

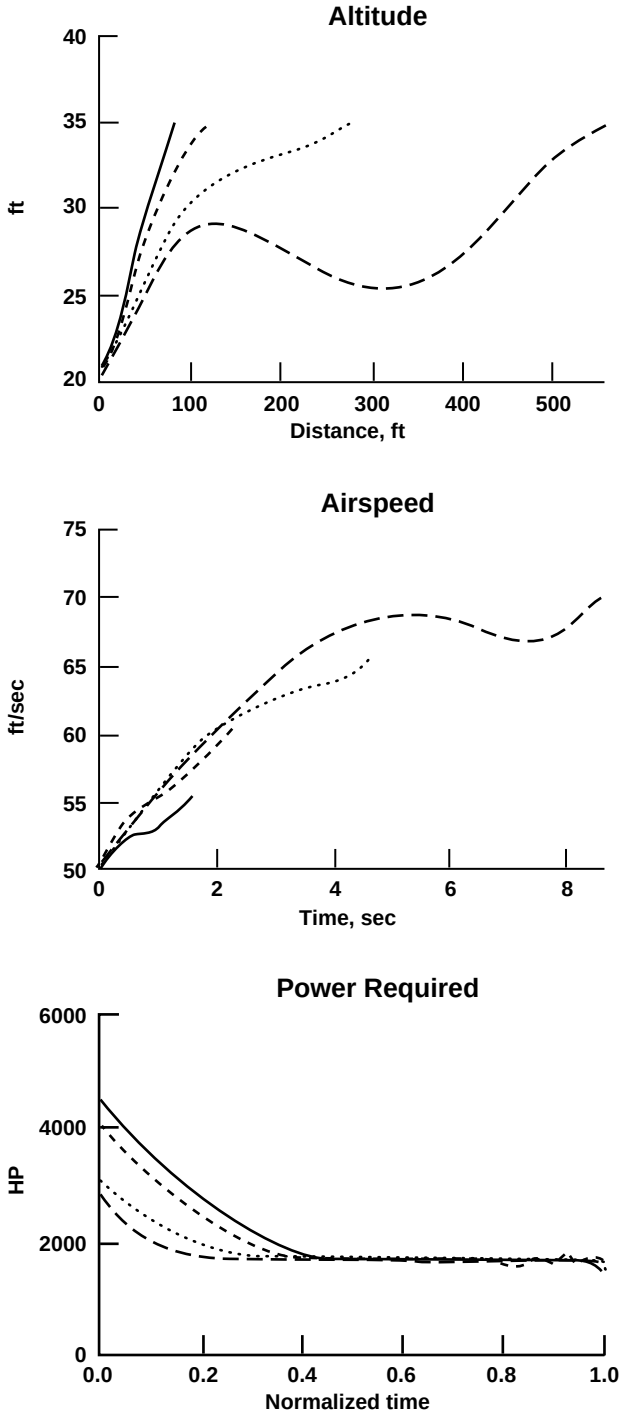

Figure 12. Effect of U_2 in OEI minimum runway-length STOL- CTO (gross weight varied with U_2 shown in table 1).

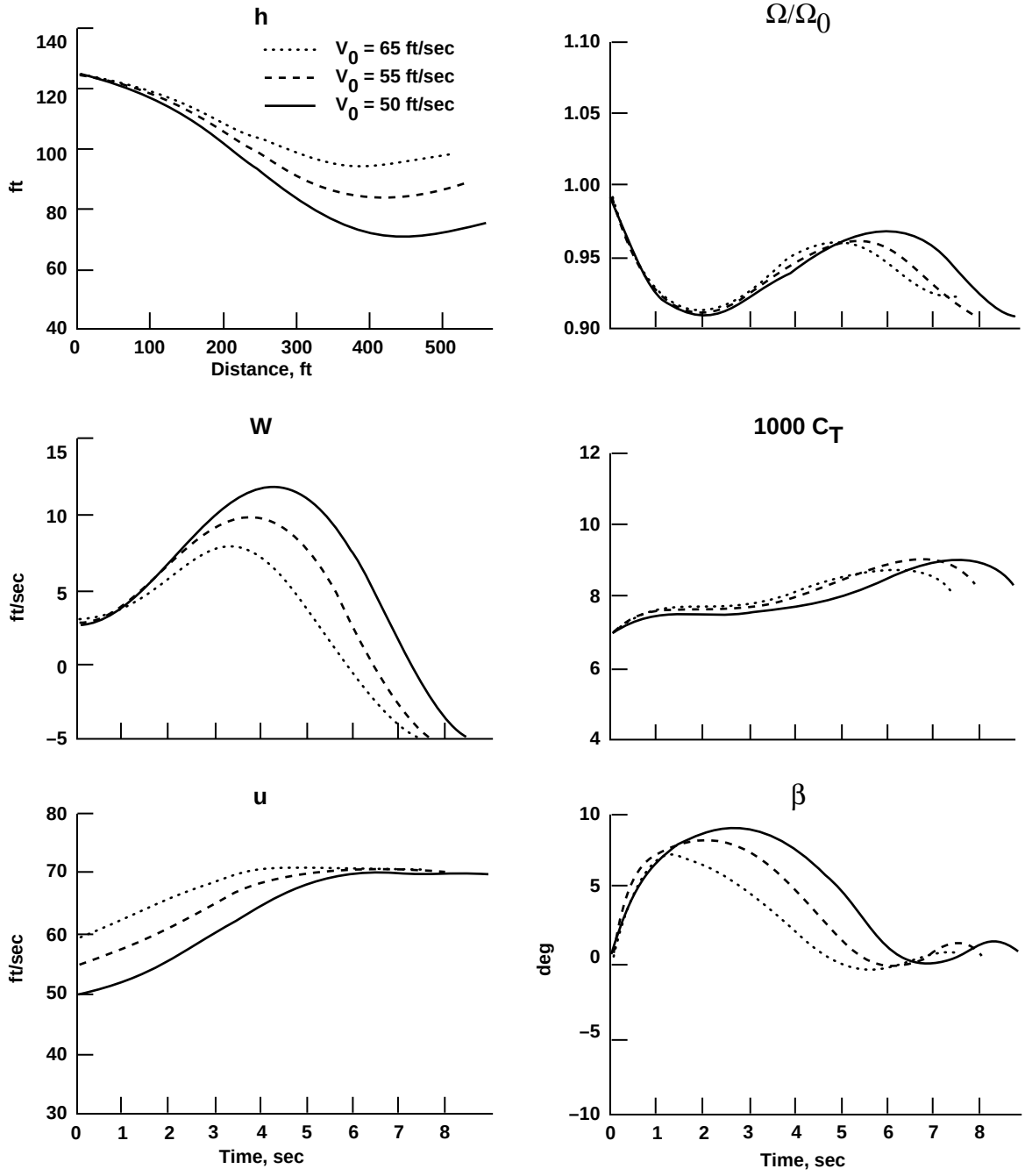

Figure 13. Minimum runway BL with different initial airspeeds: W = 19,123 lb, U_2 = 70 ft/sec, h_0 = 125 ft, and γ_0 = –3°.

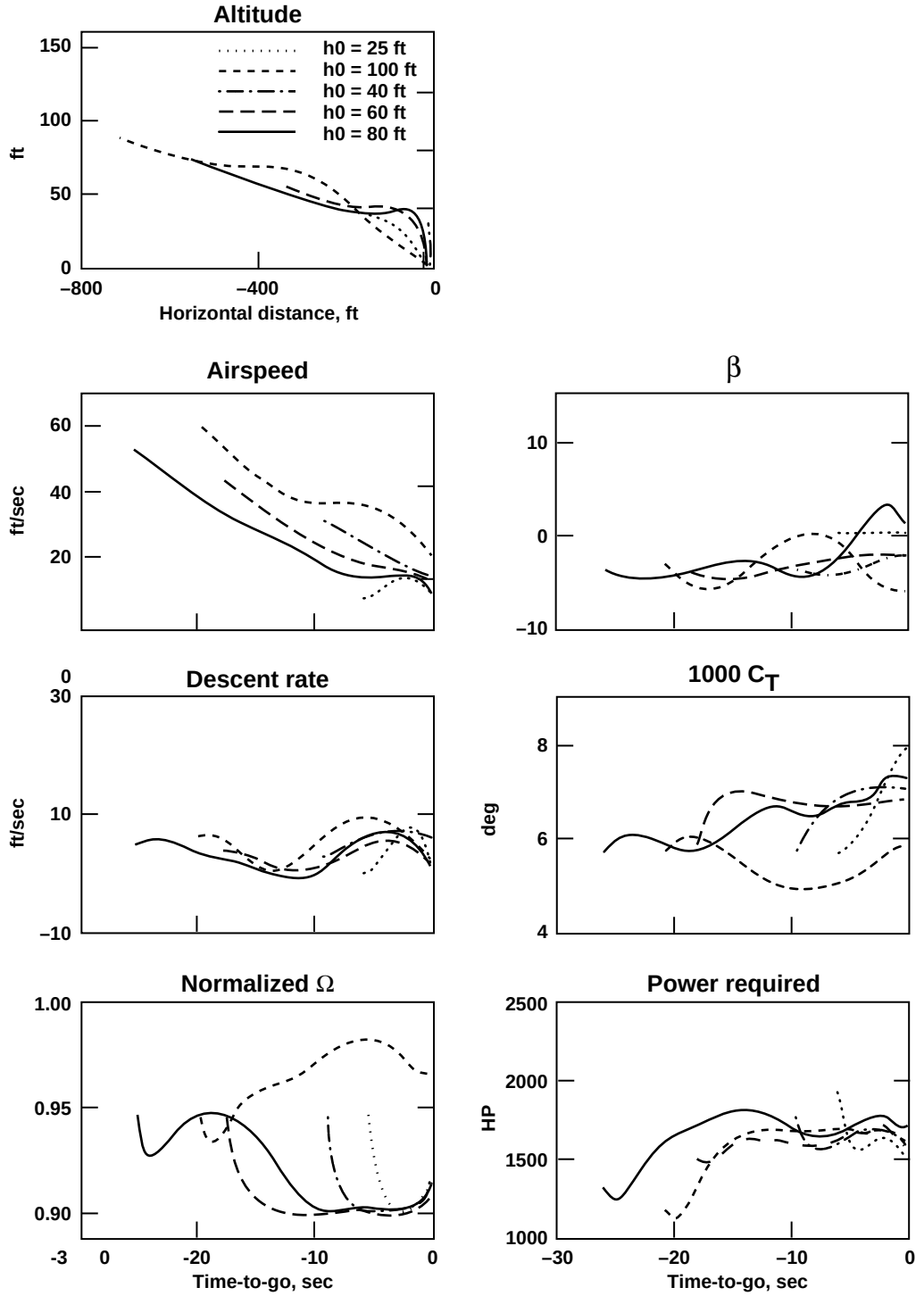

Figure 14. Effect of initial altitude on optimal VTOL-CL trajectories: W = 16,000 lb, P_{OEI} = 1656 hp, γ_0 = –6°, and V_0 varied with h_0 on the AEO landing path.

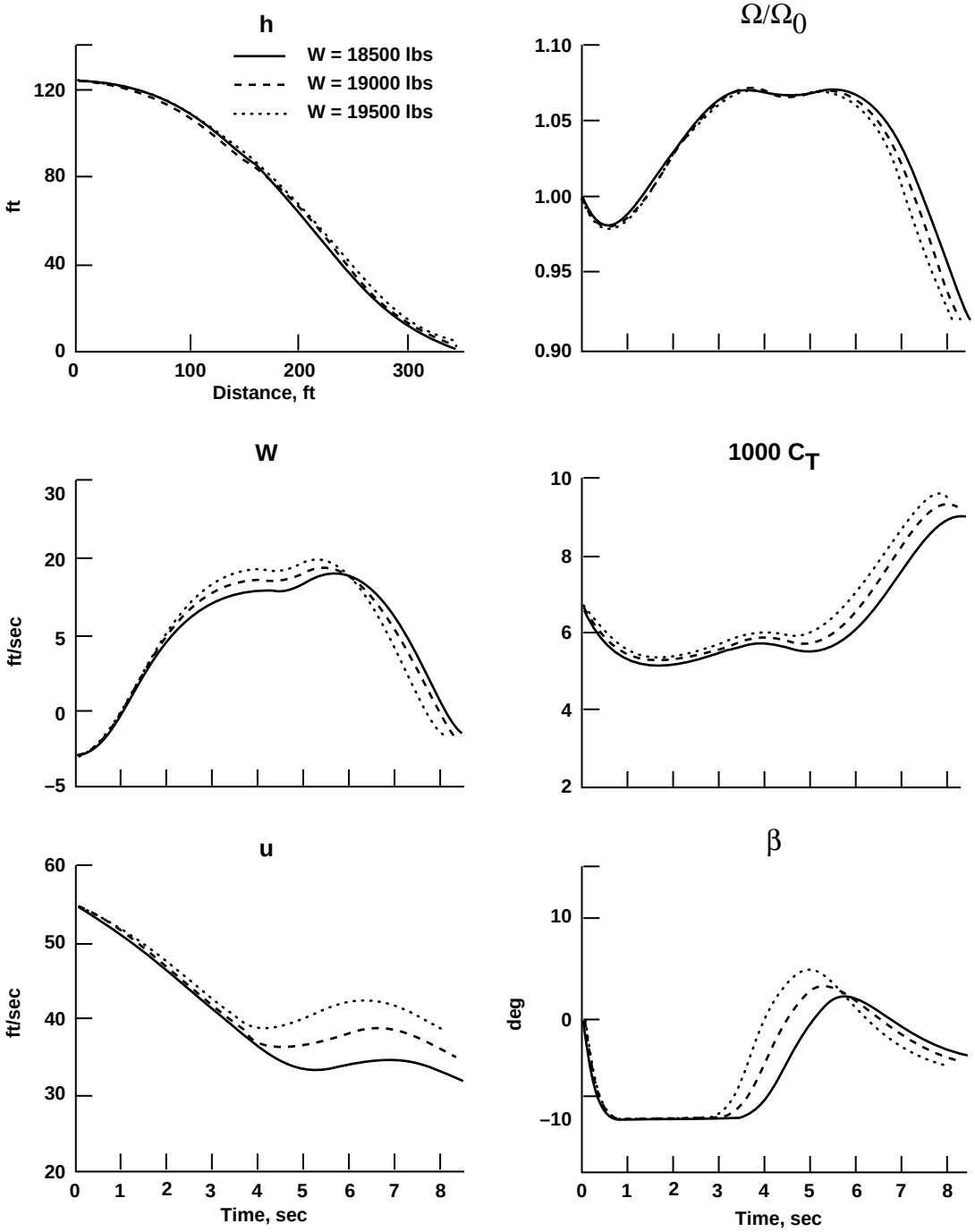

Figure 15. Effect of gross weight on minimum runway CL trajectories: h_0 = 125 ft, γ_0 = –3°, and V_0 = 55 ft/sec.

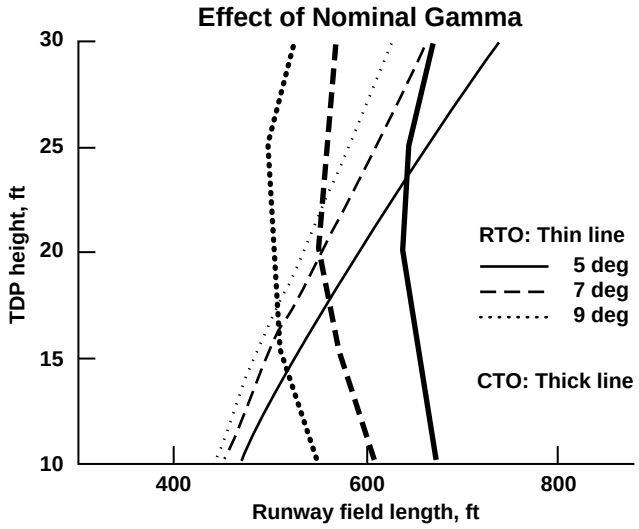

Figure 16. STOL minimum runway length for V_0 = 50 ft/sec, W = 18,610 lb, and U_2 = 65 ft/sec (for CTO).

REPORT DOCUMENTATION PAGE

Form Approved
OMB No. 0704-0188

1. AGENCY USE ONLY *(Leave blank)*	2. REPORT DATE	3. REPORT TYPE AND DATES COVERED
	May 1996	Technical Memorandum

4. TITLE AND SUBTITLE

Optimal Trajectories for the Helicopter in One-Engine-Inoperative Terminal-Area Operations

5. FUNDING NUMBERS

505-59-36

6. AUTHOR(S)

Robert T. N. Chen and Yiyuan Zhao*

7. PERFORMING ORGANIZATION NAME(S) AND ADDRESS(ES)

Ames Research Center
Moffett Field, CA 94035-1000

8. PERFORMING ORGANIZATION REPORT NUMBER

A-961613

9. SPONSORING/MONITORING AGENCY NAME(S) AND ADDRESS(ES)

National Aeronautics and Space Administration
Washington, DC 20546-0001

10. SPONSORING/MONITORING AGENCY REPORT NUMBER

NASA TM-110400

11. SUPPLEMENTARY NOTES

Point of Contact: Robert T. N. Chen, Ames Research Center, MS 211-2, Moffett Field, CA 94035-1000
(415) 604-5008
*University of Minnesota, Minneapolis, Minnesota.

12a. DISTRIBUTION/AVAILABILITY STATEMENT

Unclassified — Unlimited
Subject Category 01

12b. DISTRIBUTION CODE

13. ABSTRACT ***(Maximum 200 words)***

This paper presents a summary of a series of recent analytical studies conducted to investigate one-engine-inoperative (OEI) optimal control strategies and the associated optimal trajectories for a twin engine helicopter in Category-A terminal-area operations. These studies also examine the associated heliport size requirements and the maximum gross weight capability of the helicopter. Using an eight states, two controls, augmented point-mass model representative of the study helicopter, continued takeoff (CTO), rejected takeoff (RTO), balked landing (BL), and continued landing (CL) are investigated for both vertical-takeoff-and-landing (VTOL) and short-takeoff-and-landing (STOL) terminal-area operations. The formulation of the nonlinear optimal control problems with considerations for realistic constraints, solution methods for the two-point boundary-value problem, a new real-time generation method for the optimal OEI trajectories, and the main results of this series of trajectory optimization studies are presented. In particular, a new balanced-weight concept for determining the takeoff decision point for VTOL Category-A operations is proposed, extending the balanced-field length concept used for STOL operations.

14. SUBJECT TERMS	15. NUMBER OF PAGES
Optimal trajectory, Helicopter, One-engine-inoperative	34
	16. PRICE CODE: A03

17. SECURITY CLASSIFICATION OF REPORT	18. SECURITY CLASSIFICATION OF THIS PAGE	19. SECURITY CLASSIFICATION OF ABSTRACT	20. LIMITATION OF ABSTRACT
Unclassified	Unclassified		